



UNIVERSITY OF LEEDS

This is a repository copy of *BRAF and DIS3 Mutations Associate with Adverse Outcome in a Long-term Follow-up of Patients with Multiple Myeloma*.

White Rose Research Online URL for this paper:  
<http://eprints.whiterose.ac.uk/156311/>

Version: Supplemental Material

---

**Article:**

Boyle, EM, Ashby, C, Tytarenko, R et al. (25 more authors) (2020) BRAF and DIS3 Mutations Associate with Adverse Outcome in a Long-term Follow-up of Patients with Multiple Myeloma. *Clinical Cancer Research*, 26 (10). pp. 2422-2432. ISSN 1078-0432

<https://doi.org/10.1158/1078-0432.CCR-19-1507>

---

© 2020, American Association for Cancer Research. This is an author produced version of a paper published in *Clinical Cancer Research*. Uploaded in accordance with the publisher's self-archiving policy.

**Reuse**

Items deposited in White Rose Research Online are protected by copyright, with all rights reserved unless indicated otherwise. They may be downloaded and/or printed for private study, or other acts as permitted by national copyright laws. The publisher or other rights holders may allow further reproduction and re-use of the full text version. This is indicated by the licence information on the White Rose Research Online record for the item.

**Takedown**

If you consider content in White Rose Research Online to be in breach of UK law, please notify us by emailing [eprints@whiterose.ac.uk](mailto:eprints@whiterose.ac.uk) including the URL of the record and the reason for the withdrawal request.



[eprints@whiterose.ac.uk](mailto:eprints@whiterose.ac.uk)  
<https://eprints.whiterose.ac.uk/>

# Long-Term Follow-up Identifies That *BRAF* and *DIS3* Mutations Impact Outcome In Multiple Myeloma

## Authors

Eileen M. Boyle<sup>1,2,3\*</sup>, Cody Ashby<sup>1\*</sup>, Ruslana G. Tytarenko<sup>1</sup>, Shayu Deshpande<sup>1</sup>, Hongwei Wang<sup>4</sup>, Yan Wang<sup>1</sup>, Adam Rosenthal<sup>4</sup>, Jeffrey Sawyer<sup>1</sup>, Erming Tian<sup>1</sup>, Erin Flynt<sup>2</sup>, Antje Hoering<sup>4</sup>, Sarah K Johnson<sup>1</sup>, Michael W. Rutherford<sup>1</sup>, Christopher P Wardell<sup>1</sup>, Michael A. Bauer<sup>1</sup>, Charles Dumontet<sup>2</sup>, Thierry Facon<sup>6</sup>, Sharmilan Thanendrarajan<sup>1</sup>, Carolina D. Schinke<sup>1</sup>, Maurizio Zangari<sup>1</sup>, Frits van Rhee<sup>1</sup>, Bart Barlogie<sup>6</sup>, David Cairns<sup>8</sup>, Graham Jackson<sup>9</sup>, Anjan Thakurta<sup>4</sup>, Faith E Davies<sup>3</sup>, Gareth J Morgan<sup>3</sup>, and Brian A. Walker<sup>1</sup>

\*These authors contributed to this work equally

1. Myeloma Center, Winthrop P. Rockefeller Cancer Institute, University of Arkansas for Medical Sciences, Little Rock, AR, USA.
2. INSERM 1052/CNRS 5286 Cancer Research Center of Lyon, Lyon, FRANCE
3. Myeloma Research Program, New-York University, Langone's Perlmutter Cancer Center, New York, NY
4. Cancer Research and Biostatistics, Seattle, WA
5. Celgene Corporation, Summit, NJ
6. Service des maladies du sang. Hôpital Claude Huriez, Lille University Hospital, Lille, France
7. Department of Hematology and Medical Oncology, Tisch Cancer Institute, Icahn School of Medicine at Mount Sinai, New York, NY
8. Clinical Trials Research Unit, Leeds Institute of Clinical Trials Research
9. Northern Institute for Cancer Research, Newcastle University, Newcastle upon Tyne, UK

**Corresponding Author:** Brian A Walker

Address: Department of Hematology Oncology, Simon Cancer Center, Indiana University, Indianapolis, IN, USA

Email: [bw75@iu.edu](mailto:bw75@iu.edu)

## Index

### Supplementary methods

**Supplemental Table 1:** List of gene present on this custom targeted panel.

**Supplemental Table 2:** Comparison of Sequencing and FISH calls for deletions of 1p12, 13q, and 17p13.1 and gain/amplification of 1q21.

**Supplementary Table 3:** Copy number changes in the TT study and comparison to MGP study. \* $p < 0.05$

**Supplemental Table 4:** Incidence of the most frequently mutated genes in this TT baseline study and comparison to MGP study. \* $p < 0.05$

**Supplemental Table 5:** Univariate analysis for EFS and OS. In red all variables with  $p < 0.05$ . HR=hazard ratio, CI= confidence intervals.

**Supplemental Table 6:** Multivariate analysis for EFS.

**Supplemental Table 7:** Multivariate analysis for OS.

**Supplemental Table 8:** Justification of the classification of *BRAF* mutations.

**Supplemental Table 9:** Breakdown of patients by Total therapy trial.

**Supplemental Table 10:** Comparison of sequencing translocation calls against microarray-defined translocation groups.

**Supplemental Table 11:** Incidence of translocations in this study and in the MGP dataset.

**Supplemental Figure 1:** Summary of the Total Therapy Trials.

**Supplemental Figure 2:** Summary of sample processing.

**Supplemental Figure 3:** Validation of Mutations.

**Supplemental Figure 4:** Validation of Copy Number Metrics.

**Supplemental Figure 5:** Validation of Copy number changes (*TP53*).

**Supplemental Figure 6:** *MYC* rearrangements.

**Supplemental Figure 7:** Example of *MYC* rearrangements.

**Supplemental Figure 8:** nNMF: signatures.

**Supplemental Figure 9:** Impact of Double-Hit on outcome.

**Supplemental Figure 10:** Power analysis for EFS and OS based on group size given the 8-year follow-up.

**Supplemental Figure 11:** Impact of current survival models on outcome in this dataset.

**Supplemental Figure 12:** Impact of translocation partners in this dataset.

**Supplemental Figure 13:** Multivariate analysis using the common known risk factors.

**Supplemental Figure 14:** Multivariate analysis using the IFM model.

**Supplemental Figure 15:** Multivariate analysis using the GEP70 model.

**Supplemental Figure 16:** Impact of *BRAF* on outcome.

**Supplemental Figure 17:** Validation of mutations in the MGP complete dataset (n=1274), MGP intensively treated patients (n=340) and Myeloma XI patients only (n=463).

**Supplemental Figure 18:** Co-segregation of *BRAF*, *KRAS*, and *NRAS* mutations.

**Supplemental Figure 19:** Summary of the MAPK pathway.

**Supplemental Figure 20:** Examples of *TP53* deletions.

## Supplementary Methods

### Sample selection

A total of 223 unselected patients with paired germline and tumor DNA for whom informed consent for DNA sequencing was available were used in this study. Comparability to the general trial cohort was checked and presented in **Table 1** and **Supplemental Table 9**.

### Sample processing

CD138+ plasma cells were isolated from bone marrow aspirates by magnetic-activated cell sorting using the AutoMACS Pro (Miltenyi Biotec GmbH, Bergisch Gladbach, Germany) or RoboSep (STEMCELL Technologies, Vancouver, Canada). Plasma cell purity was determined by flow cytometry and only samples with >85% purity were used in this study. DNA from peripheral blood or CD34+ stem cell harvest was used as a matched non-tumor control sample for each patient to exclude germline variants. Nucleic acids were isolated using the AllPrep DNA/RNA or Puregene kits (Qiagen, Hilden, Germany).

### Statistical analysis

Time-to-event analysis was performed in R with all genetic events with  $n > 15$ . The Kaplan–Meier estimator was used to calculate time-to-event distributions. Stepwise Cox regression<sup>1</sup> in both directions, based on Akaike information criterion (AIC), using variables with  $p < 0.1$  on univariate, estimated the effects of significant covariates for time-to-event outcomes. When multiple features relating to the same event were present, such as del(1p) (*FAF1*) and del(1p) (*CDKN2C*), the one explaining the greatest variance was selected for the analysis. All variables with the exceptions of chromosome X copy number changes were included. The final Cox model consisted only of statistically significant factors at a level of  $p < 0.05$ . An additional bootstrap was performed using the rms package<sup>2</sup> ( $B=100$ ) and corrected indices ( $D_{xy}$  and  $r^2$ ) computed. As bivariable selection methods can induce biases we repeated the analysis using the well defined previously published consensus risk factors (ISS, t(4;14), t(14;20), del(1p), gain(1q)) and mutations. Furthermore, we attempted to show the impact of mutations on other risk models such as the IFM copy number model and GEP70.

Proportional testing: Kruskal-Wallis or Fisher's exact tests were used to compare the median of a continuous variable or the distribution of discrete variables across groups, when appropriate.

Correlation: Correlation between mutated genes and cytogenetic abnormalities was performed using the R package "stats". The covariance was computed using the Pearson method. The test statistic is based on Pearson's product moment correlation coefficient and follows a t distribution with length(x)-2 degrees of freedom assuming independent normal distributions. Correction for multiple testing was performed using the Bonferroni method. The covariance matrix was plotted using corrplot.<sup>3</sup>

Nonnegative matrix factorization: Mutational signatures were called using non-negative matrix factorization (nNMF) with counts per sample calculated for the six possible SNV types and the 16 possible 3-base sequence contexts, creating a table with 96 columns. The R package "NMF" was used for all calculations.<sup>4</sup> The number of signatures was determined by running 50 iterations of the algorithm for 2-7 signatures. A number of signatures was chosen that maximized the cophenetic distance and dispersion values. One thousand (1,000) iterations of the algorithm were run for that number of signatures. Cosine similarity was used to determine the Sanger signatures that were closest to the detected signatures.

Validation cohort: the MMRF compass prospective cohort and the Myeloma XI trial patients<sup>5,6</sup> were used as a validation cohort. As we suspected these risk factors to be associated with chemo resistance we used the subset of patients that received a stem cell transplant (n=341) and the Myeloma XI intensive subset (n=463).

### **Cohort description**

A total of 223 patients were sequenced and included in the study. The median age at diagnosis was 59 years (range: 30-75) and 64% were male (n=144). Ten percent of patients were African-American (n=22), 88% White-Caucasian (n=199) and 2% of other ethnic background. Sixteen percent were considered as high risk according to the GEP70 score and they had a worse outcome than standard risk patients both in terms of EFS (2.25 years (95% CI 1.71-6.7) versus 7.18 years (95% CI 5.6-∞), p<0.001) and OS (8y-OS 31% (17%-56%) versus 66% (59%-78%), p<0.001). Based on their ISS 26%, 43% and 30% of patients were considered Standard, Intermediate and High risk respectively with a hazard ratio of death of 2.7 ((1.2-5.9), p=0.01) and

6.1 ((2.8-13),  $p < 0.0001$ ) for ISS II and III respectively in comparison to ISS I. All patients were all included in the different total therapy trials, **Supplemental Table 9**. They were otherwise matched on age, ethnicity, ISS, and GEP70 score.

The genetic architecture of this population was overall representative of fit newly diagnosed MM patients. Hyperdiploidy was seen in 60% of cases ( $n=135$ ). The most frequent IG translocations involved *MMSET* (13.4%,  $n=30$ ) followed by *CCND1* (13%,  $n=29$ ). The *MAF* and *MAFB* translocation made up 6.7% of patients (3% and 2.7% with *MAF* and *MAFB* respectively) and *CCND3* 3.6% ( $n=8$ ). These results were in perfect accordance with the GEP based TC classification results with the exception of one t(6;14) patient, **Supplemental Table 10**. The incidence of *CCND1* translocation was smaller in this data but the overall distribution of translocation was similar, **Supplemental Table 11**.

The incidence of most copy number changes was higher for most genes in comparison to the MGP dataset. Indeed, the incidence of del(1p) [using either *FAF1*, *FAM46C* and *CDKN2C*], gain(1q) [*CKS1B*], del(11q) [*BIRC2/3*], and del(17p) [*TP53*] were significantly higher at a level of significance of 0.05, **Supplemental Table 3**. This may be explained by the methods of detection used in both dataset: in the MGP, copy number data was determined by the control FREEC tool that computes and normalizes 50kB segments for copy number. In this dataset, copy number was determined using smaller segments using two consecutive segments to define a copy number changes thus detecting interstitial deletions in genes such as *TP53* with a greater accuracy, **Supplemental Figure 20**.

**Supplemental Table 1: List of gene present on this custom targeted panel.**

<i>ARID1A</i>	<i>CHD2</i>	<i>FBXW7</i>	<i>KRAS</i>	<i>PSMG2</i>
<i>ARHGEF12</i>	<i>CHD4</i>	<i>FCHSD2</i>	<i>LRP1B</i>	<i>PTPN11</i>
<i>ARID2</i>	<i>CHEK1</i>	<i>FGFR3</i>	<i>LRRK2</i>	<i>RAD50</i>
<i>ASXL1</i>	<i>CHEK2</i>	<i>HDAC1</i>	<i>LTB</i>	<i>RB1</i>
<i>ATM</i>	<i>CRBN</i>	<i>HDAC4</i>	<i>MAF</i>	<i>RBX1</i>
<i>ATR</i>	<i>CREBBP</i>	<i>HDAC7</i>	<i>MAFB</i>	<i>SETD2</i>
<i>ATRX</i>	<i>CUL4A</i>	<i>HIST1H1C</i>	<i>MAP3K14</i>	<i>SF3B1</i>
<i>BCL10</i>	<i>CUL4B</i>	<i>HIST1H1D</i>	<i>MAX</i>	<i>SMARCA4</i>
<i>BCL6</i>	<i>CXCR4</i>	<i>HIST1H1E</i>	<i>MKI67</i>	<i>STAT3</i>
<i>BCL7A</i>	<i>CYLD</i>	<i>IDH1</i>	<i>MLL</i>	<i>TAF1</i>
<i>BCORL1</i>	<i>DDB1</i>	<i>IDH2</i>	<i>MYC</i>	<i>TET1</i>
<i>BIRC2</i>	<i>DIS3</i>	<i>IKZF1</i>	<i>MYD88</i>	<i>TET2</i>
<i>BIRC3</i>	<i>DNMT3A</i>	<i>IKZF3</i>	<i>NCKAP5</i>	<i>TET3</i>
<i>BRAF</i>	<i>DOT1L</i>	<i>IKZF4</i>	<i>NCOR1</i>	<i>TP53</i>
<i>BRCA1</i>	<i>EGFR</i>	<i>IRF4</i>	<i>NEDD9</i>	<i>TRAF2</i>
<i>BRCA2</i>	<i>EGR1</i>	<i>JAK1</i>	<i>NF1</i>	<i>TRAF3</i>
<i>BRD4</i>	<i>EP300</i>	<i>JAK2</i>	<i>NOTCH1</i>	<i>U2AF1</i>
<i>BRF1</i>	<i>EZH1</i>	<i>JAK3</i>	<i>NOTCH4</i>	<i>VSIG6</i>
<i>CARD11</i>	<i>EZH2</i>	<i>KAT6A</i>	<i>NR3C1</i>	<i>WHSC1</i>
<i>CCND1</i>	<i>FAF1</i>	<i>KDM2B</i>	<i>NRAS</i>	<i>WHSC1L1</i>
<i>CCND3</i>	<i>FAM46C</i>	<i>KDM5A</i>	<i>PCLO</i>	<i>XBP1</i>
<i>CD36</i>	<i>FANCA</i>	<i>KDM6A</i>	<i>POT1</i>	<i>ZFHX4</i>
<i>CDKN1B</i>	<i>FANCD2</i>	<i>KMT2B</i>	<i>PRDM1</i>	<i>ZRSR2</i>
<i>CDKN2C</i>	<i>FANCI</i>	<i>KMT2C</i>	<i>PRKD2</i>	
<i>CHD1</i>	<i>FANCM</i>	<i>KMT2D</i>	<i>PSMB5</i>	

**Supplemental Table 2: Comparison of Sequencing and FISH calls for deletions of 1p12, 13q, and 17p13.1 and gain/amplification of 1q21.**

Sequencing	FISH (20% cut-off)		
<b>del1p (n=166)</b>	del1p13*	normal	
<b>Del1p12 (FAM46C)</b>	22	11	sensitivity = 84.62% (95% CI 65.13-95.64)
<b>normal</b>	4	129	specificity = 92.14% (95% CI 86.38-96.01)
<b>gain1q (n=166)</b>	gain/amp CKS1B	normal	
<b>gain/amp1q (1q21.3)</b>	58	1	sensitivity = 80.56% (95% CI 69.53-88.94)
<b>normal</b>	14	93	specificity = 98.94% (95% CI 94.21-99.97)
<b>amp1q (n=166)</b>	amp CKS1B	not amp	
<b>amp1q (1q21.3)</b>	9	1	sensitivity = 36.00% (95% CI 17.97-57.48)
<b>not amp</b>	16	140	specificity = 99.29% (95% CI 96.11-99.98)
<b>del13q (n=66)</b>	del13q (D13S31)	normal	
<b>del13q (RB1)</b>	32	1	sensitivity = 94.12% (95% CI 80.32-99.28)
<b>normal</b>	2	31	specificity = 96.88% (95% CI 83.78-99.92)
<b>del17p (n=158)</b>	del17p (TP53)	normal	
<b>delTP53</b>	14	3	sensitivity = 77.78% (95% CI 52.36-93.59)
<b>normal</b>	4	137	specificity = 97.86% (95% CI 93.87-99.56)

\*1p probe is at 1p13 and is compared to *FAM46C* at 1p12.

**Supplemental Table 3: Copy number changes in the Baseline study and comparison to MGP dataset. \*p<0.05**

Gene	Percentage in this study (n=223)	Percentage in MGP (n=784)	Chi-statistic, p-value
<b>del(1p): <i>FAM46C</i></b>	23% (n=51/223)	15% (n=116/784)	$\chi^2=7.6$ , p=0.006
<b>del(1p): <i>CDKN2C</i></b>	17% (n=38/223)	9% (n=74/784)	$\chi^2=10.1$ , p=0.002
<b>del(1p): <i>FAF1</i></b>	17% (n=38/223)	9% (n=74/784)	$\chi^2=10.1$ , p=0.002
<b>amp(1q): <i>CKS1B</i></b>	5% (n=12/223)	9% (n=53/784)	$\chi^2=0.45$ , p=0.56
<b>gain(1q): <i>CKS1B</i></b>	30% (n=68/223)	22% (n=173/784)	$\chi^2=6.31$ , p=0.012
<b>del(6q): <i>PARK2</i></b>	15% (n=34/223)	15% (n=119/784)	$\chi^2=0.006$ , p=0.98
<b>del(11q): <i>BIRC2/3</i></b>	5% (n=11/223)	3% (n=20/784)	$\chi^2=3.3$ , p=0.07
<b>del(12p): <i>CDKN1B</i></b>	9% (n=20/223)	9% (n=71/784)	$\chi^2=0.002$ , p=1
<b>del(13q): <i>DIS3</i></b>	46% (n=103/223)	40% (n=317/784)	$\chi^2=2.7$ , p= 0.094
<b>del(13q): <i>RB1</i></b>	50% (n=111/223)	44% (n=343/784)	$\chi^2=2.3$ , p=0.12
<b>del(14q): <i>TRAF3</i></b>	22% (n=48/223)	16% (n=129/784)	$\chi^2=3.1$ , p=0.1
<b>del(16q): <i>CYLD</i></b>	26% (n=58/223)	21% (n=166/784)	$\chi^2=2.34$ , p=0.13
<b>del(17p): <i>TP53</i></b>	17% (n=38/223)	8% (n=63/784)	$\chi^2=15.6$ p=0.0001.

**Supplemental Table 4: Incidence of the most frequently mutated genes in this TT baseline study and comparison to MGP study. \*p<0.05**

<b>Gene</b>	<b>Percentage in this study (n=223)</b>	<b>Percentage in MGP (n=1273)</b>
<i><b>KRAS</b></i>	22.87%	21.84%
<i><b>NRAS</b></i>	17.04%	17.44%
<i><b>BRAF</b></i>	11.66%	8.01%
<i><b>DIS3</b></i>	9.42%	9.98%
<i><b>TP53</b></i>	7.62%	5.66%
<i><b>TRAF3</b></i>	7.62%	5.26%
<i><b>FAM46C</b></i>	7.17%	9.35%
<i><b>LRP1B</b></i>	5.83%	7.31%
<i><b>LRRK2</b></i>	5.83%	1.18%*
<i><b>CYLD</b></i>	5.38%	3.38%
<i><b>ATM</b></i>	4.48%	4.32%
<i><b>ZFHX4</b></i>	4.48%	4.70%

**Supplemental Table 5: Univariate analysis for EFS and OS. In red all variables with p<0.05. HR=hazard ratio, CI= confidence intervals.**

Covariate	EFS		OS	
	HR (95% CI for HR)	p-value	HR (95% CI for HR)	p-value
Double hit	4.6 (2.7-7.9)	<0.0001	3.5 (1.9-6.5)	<0.0001
Biallelic <i>TP53</i>	4.3 (2.4-7.7)	<0.0001	2.8 (1.4-5.6)	0.004
High GEP70	2.5 (1.6-3.9)	<0.0001	3.5 (2.1-6)	<0.0001
Bi-allelic <i>DIS3</i>	3.6 (1.8-7.2)	0.00033	2.2 (0.89-5.6)	0.088
<i>ISS3</i>	2 (1.4-3)	0.00027	3 (1.9-4.7)	<0.0001
del(17p): <i>TP53</i>	2.3 (1.5-3.6)	0.0015	1.8 (1.3-3.3)	0.034
<i>ISS1</i>	0.48 (0.29-0.78)	0.0036	0.26 (0.12-0.53)	0.00028
Gain or amp(1q)	1.8 (1.2-2.6)	0.0037	2.3 (1.4-3.5)	0.00043
Trisomy 9	0.58 (0.4-0.84)	0.0042	0.54 (0.35-0.85)	0.0078
Gain 8q	2.3 (1.3-4.1)	0.003	2.9 (1.5-5.5)	0.0012
<i>TP53</i>	2.3 (1.3-4.2)	0.0065	1.5 (0.67-3.2)	0.34
Trisomy 19	0.75 (0.63-0.9)	0.0022	0.65 (0.53-0.79)	<0.0001
<i>BRAF</i>	2 (1.2-3.3)	0.0094	2.7 (1.5-4.7)	0.00076
<i>DIS3</i>	2 (1.2-3.4)	0.0096	1.2 (0.56-2.4)	0.68
PR subgroup GEP	1.9 (1.1-3.1)	0.0096	2.5 (1.5-4.4)	0.00085
gain(1q)	1.6 (1.1-2.3)	0.02	1.9 (1.2-3)	0.0056
<i>MMSET</i> translocation	1.8 (1.2-2.9)	0.0092	1.6 (0.94-2.8)	0.082
MF cluster	2.4 (1.2-4.7)	0.015	2.1 (0.96-4.6)	0.063
del(1p): <i>FAF1</i>	1.8 (1.1-2.8)	0.018	1.9 (1.1-3.3)	0.018
Trisomy 19: <i>KMT2B</i>	0.64 (0.44-0.94)	0.023	0.56 (0.35-0.9)	0.016
del(1p): <i>CDKN2C</i>	1.7 (1.1-2.7)	0.023	1.9 (1.1-3.2)	0.022
del(12p): <i>KDM5A</i>	1.9 (1.1-3.5)	0.026	2.6 (1.4-4.9)	0.0024
Trisomy 19: <i>PRKD2</i>	0.66 (0.45-0.97)	0.035	0.61 (0.38-0.97)	0.036
DNA repair mutations	2 (1.1-4.1)	0.023	2.2 (1.1-4.6)	0.033
Trisomy 5	0.67 (0.46-0.98)	0.037	0.83 (0.53-1.3)	0.41
MS cluster by GEP	1.7 (1-2.7)	0.034	1.4 (0.82-2.5)	0.21
del(1p): <i>FAM46C</i>	1.5 (0.99-2.3)	0.061	1.6 (1-2.7)	0.051
del(13q): telomere	1.4 (0.97-2.1)	0.072	1.7 (1-2.6)	0.03
amp(1q)	1.9 (0.89-4.2)	0.096	2.6 (1.1-6)	0.026
Monoallelic <i>DIS3</i>	1.2 (0.85-1.8)	0.27	1.2 (0.74-1.8)	0.53
<i>MYC</i> deletion	1.4 (0.88-2.3)	0.15	1.8 (1-3.1)	0.043
Trisomy 3	0.75 (0.51-1.1)	0.14	0.84 (0.53-1.3)	0.44
del(13q): centromere	1.3 (0.88-1.9)	0.19	1.6 (0.99-2.4)	0.056
del(17p): telomere	1.4 (0.79-2.3)	0.27	1.2 (0.6-2.3)	0.64
<i>MYC</i> translocation	0.77 (0.49-1.2)	0.26	1.1 (0.65-1.8)	0.7
<i>CYLD</i>	1.4 (0.61-3.2)	0.6	1.4 (0.58-3.6)	0.59
Trisomy 15	0.87 (0.6-1.3)	0.47	0.76 (0.48-1.2)	0.23
<i>MYC</i> gain	1.1 (0.73-1.7)	0.64	1.7 (1.1-2.7)	0.03
<i>NRAS</i>	0.88 (0.52-1.5)	0.65	0.98 (0.53-1.8)	0.96
Trisomy 21	0.92 (0.6-1.4)	0.17	1.2 (0.73-1.9)	0.45
<i>ISS2</i>	0.92 (0.63-1.3)	0.66	0.84 (0.53-1.3)	0.46
<i>KRAS</i>	0.99 (0.63-1.6)	0.96	1.1 (0.63-1.9)	0.79
<i>TRAF3</i>	0.99 (0.48-2)	0.98	1.2 (0.51-2.7)	0.7

**Supplemental Table 6: Multivariate analysis for EFS. Multivariate model uses stepwise selection with entry level 0.1 and variable remain if meets the 0.05 level.**

	<b>n/N</b>	<b>Coef</b>	<b>S.E.</b>	<b>Wald</b>	<b>Pr(&gt; Z )</b>
<b>Double-Hit</b>	19/223	1.2592	0.2984	4.22	<0.0001
<b>Trisomy 19</b>	92/223	-0.5467	0.2208	-2.475	0.013307
<b>BRAF</b>	26/223	0.6361	0.3213	1.98	0.047723
<b>DIS3</b>	21/223	0.5447	0.259	2.103	0.035474
<b>t(4;14)</b>	32/223	0.6983	0.2555	2.733	0.006283
<b>del(1p): <i>FAF1</i></b>	38/223	1.1822	0.2908	4.065	<0.0001
<b>del(12p) <i>KDM5A</i></b>	19/223	0.9837	0.2953	3.332	0.000864
Concordance= 0.689 (se = 0.027 ), r <sup>2</sup> = 0.223 (max possible= 0.991 ), Likelihood ratio test= 56.99 on 7 df, p=6e <sup>-10</sup> , Wald test= 62.03 on 7 df, p=6e <sup>-11</sup> , Score (logrank) test = 72.96 on 7 df, p=4e <sup>-13</sup>					

**Supplemental Table 7: Multivariate analysis for OS Multivariate model uses stepwise selection with entry level 0.1 and variable remain if meets the 0.05 level.**

	<b>n/N</b>	<b>Coef</b>	<b>S.E.</b>	<b>Wald</b>	<b>Pr(&gt; Z )</b>
<b>Double-Hit</b>	19/223	0.7258	2.0664	0.3559	2.04
<b><i>BRAF</i></b>	26/223	-1.0758	0.341	0.2853	-3.771
<b>Trisomy 19</b>	92/223	0.9501	2.586	0.352	2.699
<b>del(12p): <i>KDM5A</i></b>	19/223	0.6879	1.9896	0.2912	2.363
<b>del(1p): <i>FAF1</i></b>	38/223	1.485	4.4151	0.3138	4.732
<b><i>MYC</i> gain</b>	63/223	0.7724	2.165	0.2555	3.024
Concordance= 0.73 (se = 0.032 ) r <sup>2</sup> = 0.22 (max possible= 0.962 ) Likelihood ratio test= 52.7 on 6 df, p=1e <sup>-09</sup> Wald test = 55.11 on 6 df, p=4e <sup>-10</sup> Score (logrank) test = 62.33 on 6 df, p=2e <sup>-11</sup>					

**Supplemental Table 8: Justification of the classification of *BRAF* mutations. A. Activating, B. Low or no kinase, C. Unknown**

**A.**

<b>Protein</b>	<b>Description</b>
<b>E586K</b>	<i>BRAF</i> E586K lies within the protein kinase domain of the <i>BRAF</i> protein (UniProt.org). E586K results in increased <i>BRAF</i> kinase activity, and activation of Mek and Erk in cell culture (PMID: 15035987, PMID: 22510884), and increases cell proliferation and viability compared to wild-type <i>BRAF</i> in one of two cell lines (PMID: 29533785).
<b>G464R</b>	<i>BRAF</i> G464R lies within the protein kinase domain of the <i>BRAF</i> protein (UniProt.org). G464R results in increased <i>BRAF</i> kinase activity, increased downstream Erk signaling (PMID: 15046639), and induces cell proliferation and cell viability in culture (PMID: 29533785).
<b>G469A</b>	<i>BRAF</i> G469A is a hotspot mutation within the protein kinase domain of the <i>BRAF</i> protein (UniProt.org). G469A results in increased <i>BRAF</i> kinase activity and downstream activation of Erk, and is transforming in cell culture (PMID: 19010912, PMID: 12068308, PMID: 29533785).
<b>G469V</b>	<i>BRAF</i> G469V is a hotspot mutation within the protein kinase domain of the <i>BRAF</i> protein (UniProt.org). G469V results in increased <i>BRAF</i> kinase activity and activation of downstream MEK and ERK in cell culture (PMID: 28947956, PMID: 26343582, PMID: 28783719), and in one of two cell lines, increased cell proliferation and cell viability compared to wild-type <i>BRAF</i> (PMID: 29533785).
<b>K601E</b>	<i>BRAF</i> K601E lies within the activation segment in the kinase domain of the <i>BRAF</i> protein (PMID: 15343278). K601E results in increased <i>BRAF</i> kinase activity and downstream activation of MEK and ERK in cell culture (PMID: 22798288, PMID: 28783719) and induces cell proliferation and cell viability in culture (PMID: 29533785).
<b>L597R</b>	<i>BRAF</i> L597R lies within the protein kinase domain of the <i>BRAF</i> protein (UniProt.org). L597R results in activation of <i>BRAF</i> as indicated by increased phosphorylation of Mek and Erk in cell culture (PMID: 22798288, PMID: 26343582), is associated with Erk activation in a patient tumor sample (PMID: 23715574), and in one of two cell lines, increased cell proliferation and cell viability compared to wild-type <i>BRAF</i> (PMID: 29533785).
<b>N486_P490del</b>	<i>BRAF</i> N486_P490del results in the deletion of five amino acids near the alphaC-helix region of the kinase domain (PMID: 26732095). N486_P490del confers a gain of function to the <i>BRAF</i> protein as indicated by activation of the MAPK signaling pathway and increased cell proliferation in culture (PMID: 26732095).
<b>V600E</b>	<i>BRAF</i> V600E lies within the activation segment of the kinase domain of the <i>BRAF</i> protein (PMID: 15035987). V600E confers a gain of function to the <i>BRAF</i> protein as demonstrated by increased <i>BRAF</i> kinase activity, downstream signaling, and the ability to transform cells in culture (PMID: 15035987, PMID: 29533785).
<b>G469R</b>	<i>BRAF</i> G469R is a hotspot mutation within the protein kinase domain of the <i>BRAF</i> protein (UniProt.org). G469R demonstrates intermediate <i>BRAF</i> kinase activity (PMID: 28783719) and results in constitutive ERK activation in cell culture (PMID: 24920063), and in one of two cell lines leads to increased cell proliferation and cell viability compared to wild-type <i>BRAF</i> (PMID: 29533785), and is therefore predicted to confer a gain of function to the <i>BRAF</i> protein.

**B.**

<b>Protein</b>	<b>Description</b>
<b>D594E</b>	BRAF D594E lies within the protein kinase domain of the Braf protein (UniProt.org). D594E results in impaired Braf kinase activity, however, results in increased Mek and Erk phosphorylation in the presence of CRAF in cell culture (PMID: 28783719).
<b>G466V</b>	BRAF G466V lies within the protein kinase domain of the Braf protein (UniProt.org). G466V results in impaired Braf kinase activity, but paradoxically activates MEK and ERK through transactivation of CRAF in cell culture (PMID: 22649091, PMID: 28783719), and in one of two cell lines, G466V decreased cell proliferation and cell viability as compared to wild-type Braf (PMID: 29533785).
<b>D594N</b>	BRAF D594N lies within the protein kinase domain of the Braf protein (UniProt.org). D594N results in impaired Braf kinase activity, but leads to activation of Erk signaling through CRAF in cell culture (PMID: 28783719), and demonstrates decreased transforming ability compared to wild-type Braf in one of two cell lines in culture (PMID: 29533785), and therefore is predicted to confer a loss of function to the Braf protein.
<b>G466R</b>	BRAF G466R (previously reported as G465R) lies within the glycine-rich loop in the protein kinase domain of the Braf protein (PMID: 14681681). G466R results in impaired Braf kinase activity, but activates Erk signaling in cell culture (PMID: 15046639), and in one of two cell lines, G466R decreased cell proliferation and cell viability compared to wild-type Braf (PMID: 29533785), and is therefore predicted to confer a loss of function
<b>G596R</b>	BRAF G596R lies within the protein kinase domain of the Braf protein, within the DFG motif (PMID: 19735675). G596R results in impaired Braf kinase activity and decreased Mek and Erk phosphorylation, including in the presence of BRAF V600E, is not transforming in culture and does not promote tumor formation in mouse models, but results in activation of Erk in the presence of CRAF (PMID: 19735675, PMID: 28783719), however, in another study demonstrates similar cell proliferation and viability levels to wild-type Braf (PMID: 29533785), and is predicted to confer a loss of function to the Braf protein.
<b>G596V</b>	BRAF G596V lies within the protein kinase domain of the Braf protein (UniProt.org). G596V results in impaired Braf kinase activity and does not activate downstream MEK and ERK in cell culture (PMID: 16439621), but leads to activation of ERK in zebrafish models (PMID: 19376813), and is therefore predicted to lead to a loss of function.
<b>N581K</b>	BRAF N581K lies within the protein kinase domain of the Braf protein (UniProt.org). N581K has not been biochemically characterized, but demonstrates decreased transformation ability in cell culture (PMID: 29533785), and is therefore predicted to confer a loss of function to the Braf protein.
<b>D594G</b>	BRAF D594G lies within the protein kinase domain of the Braf protein (UniProt.org). D594G has been demonstrated to result in impaired Braf kinase activity, but leads to increased activation of Erk signaling through CRAF in cell culture (PMID: 18794803, PMID: 28783719), however, has increased transforming ability in one of two cell lines in culture (PMID: 29533785), and therefore its effect on Braf protein function is unknown.
<b>G466A</b>	BRAF G466A (also reported as G465A) lies within the protein kinase domain of the Braf protein (UniProt.org). The functional effect of G466A on Braf is unclear as it has been characterized both as having intermediate Braf kinase activity (PMID: 15035987) and low Braf kinase activity (PMID: 28783719), leads to Ras-dependent activation of downstream Erk in cell culture (PMID: 28783719), and in one of two cell lines increased cell proliferation and cell viability compared to wild-type Braf (PMID: 29533785).
<b>G466E</b>	BRAF G466E lies within the protein kinase domain of the Braf protein (UniProt.org). G466E results in impaired Braf kinase activity, but paradoxically increases Erk signaling through C-raf activation in cell culture and Xenopus embryos (PMID: 15035987).
<b>G469E</b>	BRAF G469E is a hotspot mutation within the protein kinase domain of the Braf protein (UniProt.org). The functional effect of G469E on Braf is unclear as it has been characterized as having both low Braf kinase activity (PMID: 28783719) and intermediate Braf kinase activity (PMID: 15035987), results in Ras-dependent activation of ERK signaling in cell culture (PMID: 28783719), and in one of two cell lines, G469E increased cell proliferation and cell viability as compared to wild-type Braf (PMID: 29533785).
<b>N581I</b>	BRAF N581I lies within the protein kinase domain of the Braf protein (UniProt.org). N581I results in low Braf kinase activity and Ras-dependent activation of Erk signaling in cell culture (PMID: 28783719) but, induces similar cell proliferation and cell viability as wild-type Braf (PMID: 29533785).
<b>N581S</b>	BRAF N581S lies within the protein kinase domain of the Braf protein (UniProt.org). N581S has been demonstrated to result in intermediate Braf kinase activity (PMID: 15035987), as well low Braf kinase activity (PMID: 28783719), and results in Ras-dependent activation of ERK signaling in cell culture (PMID: 28783719), however in another study, N581S demonstrated increased transformation ability in one of two different cell lines as compared to wild-type Braf (PMID: 29533785).

**C.**

<b>Protein</b>	<b>Description</b>
<b>G596S</b>	BRAF G596S lies within the protein kinase domain of the Braf protein (UniProt.org). G596S has not been biochemically characterized, but results in increased transformation ability compared to wild-type Braf in one of two different cell lines in culture (PMID: 29533785).
<b>K483E</b>	BRAF K483E lies within the protein kinase domain of the Braf protein (UniProt.org). K483E has not been biochemically characterized, but results in increased transformation ability compared to wild-type Braf in one of two cell lines in culture (PMID: 29533785).
<b>L597P</b>	BRAF L597P lies within the protein kinase domain of the Braf protein (UniProt.org). L597P has been identified in sequencing studies (PMID: 24714776), but has not been biochemically characterized and therefore, its effect on Braf protein function is unknown.
<b>C532Y</b>	NA
<b>E501A</b>	NA
<b>G392E</b>	NA
<b>I554T</b>	NA
<b>I77K</b>	NA
<b>K483Q</b>	NA
<b>M668I</b>	NA
<b>N73T</b>	NA
<b>P403H</b>	NA
<b>Q359P</b>	NA
<b>R662G</b>	NA
<b>T119I</b>	NA
<b>T241M</b>	NA

**Supplemental Table 9: Breakdown of patients by Total therapy trial.**

	<b>223-baseline study</b>	<b>Combined TT3a-3b-4-4like-5a-5b-6</b>
<b>TT3a</b>	18.67% (n=42)	26.56% (n=276)
<b>TT3b</b>	18.67%(n=42)	16.17 % (n=168)
<b>TT4</b>	42.22%(n=95)	34.94 % (n=363)
<b>TT4-Like</b>	0.90%(n=2)	1.06 % (n=11)
<b>TT5a</b>	5.33% (n=12)	7.12 % (n=74)
<b>TT5b</b>	5.28% (n=12)	1.54 % (n=16)
<b>TT6</b>	8.00% (n=18)	12.61 % (n=131)

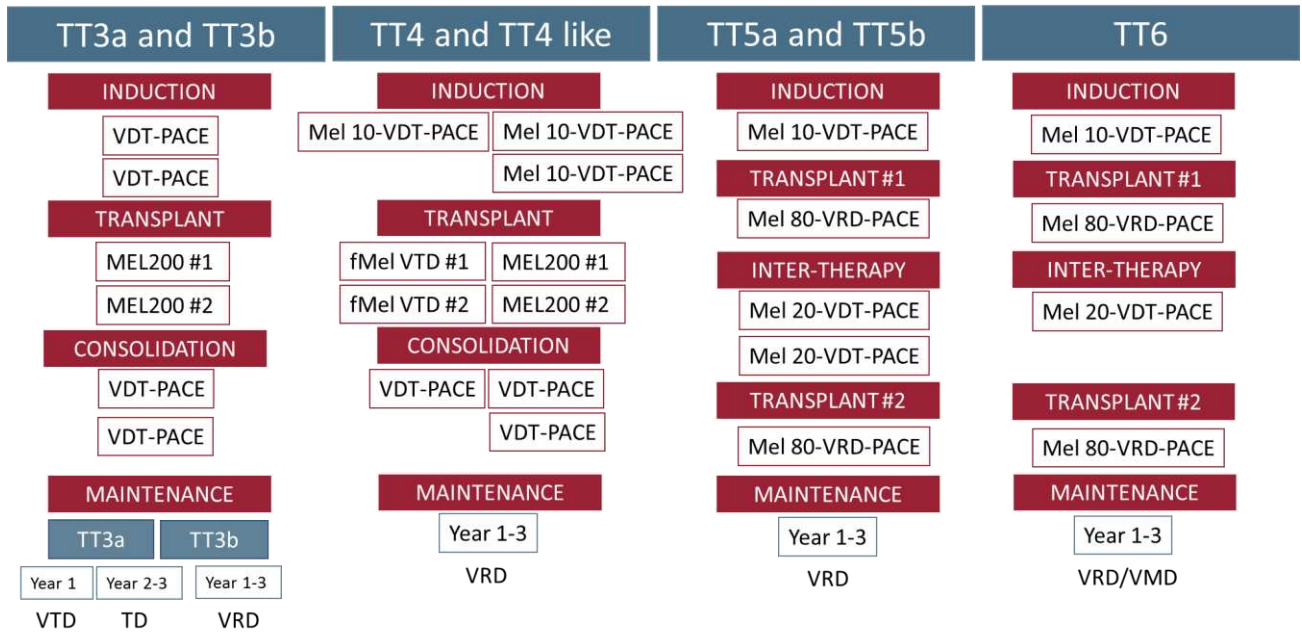
**Supplementary Table 10: Comparison of sequencing translocation calls against microarray-defined translocation groups.**

Sequencing	GEP					
	t(4;14)	t(6;14)	t(11;14)	t(14;16)	t(14;20)	None
t(4;14)	32	0	0	0	0	0
t(6;14)	0	7	0	0	0	1
t(11;14)	0	0	29	0	0	0
t(14;16)	0	0	0	9	0	0
t(14;20)	0	0	0	0	6	0
None	0	1	0	0	0	140
<b>Sensitivity:</b>	100%	87.5%	100%	100%	100%	99.2%
<b>Specificity:</b>	100%	100%	100%	100%	100%	100%

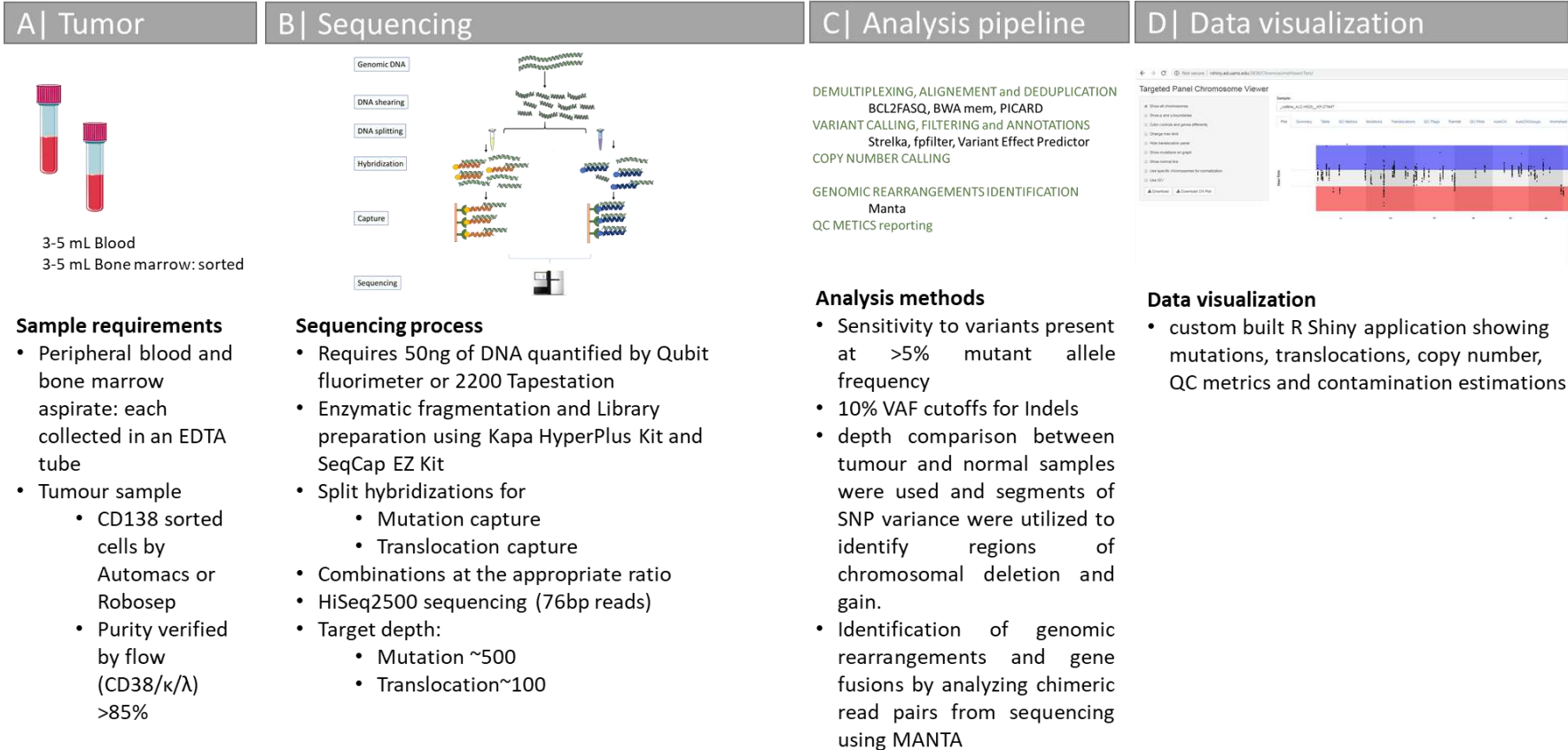
**Supplemental Table 11: Incidence of translocations in this study and in the MGP dataset.**

<b>Gene</b>	<b>Percentage in this study (n=223)</b>	<b>Percentage in MGP (n=1273)</b>	<b>p-value</b>
<b><i>CCND1</i></b>	13% (n=29/223)	18% (n=234/1273)	p=0.051
<b><i>CCDN3</i></b>	3.5% (n=8/223)	1% (n=14/1273)	p=0.005
<b><i>MAF or MAFB</i></b>	6.6% (n=15/223)	5% (n=62/1273)	p= 0.24
<b><i>MMSET</i></b>	14% (n=30/223)	12% (n=155/1273)	p=0.60

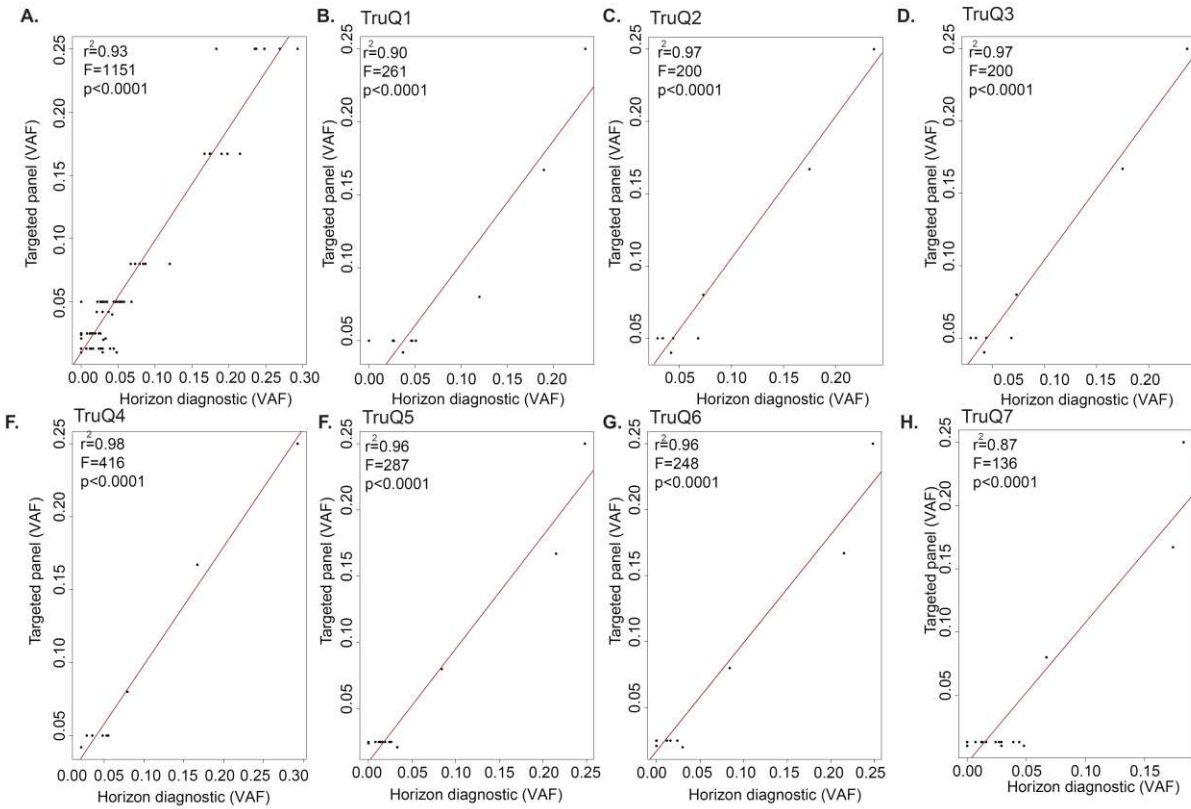
**Supplemental Figure 1: Summary of the Total Therapy Trials.** V= bortezomib, D=dexamethasone, T=thalidomide, P=cisplatin, A=doxorubicine, C=cyclophosphamide, E=etoposide, R=lenalidomide, M=melphalan, MEL= high dose melphalan, fMel=fractionated melphalan.



## Supplemental Figure 2: Summary of sample processing.

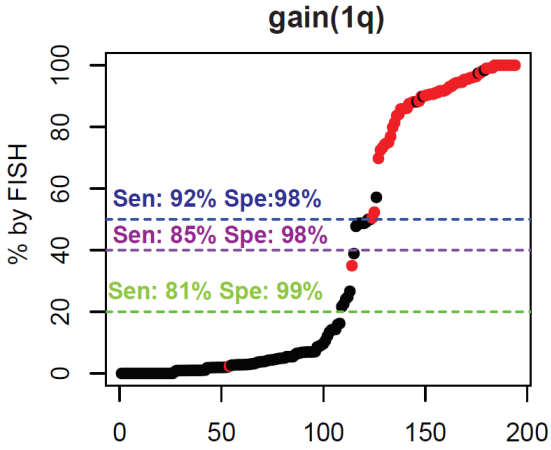


**Supplemental Figure 3: Validation of Mutations.** All mutations with VAF  $\geq 5\%$  were found on the targeted panel with a good overall correlation ( $r^2=0.93$ ) A. All samples combined, B-H. Individual reference standard.

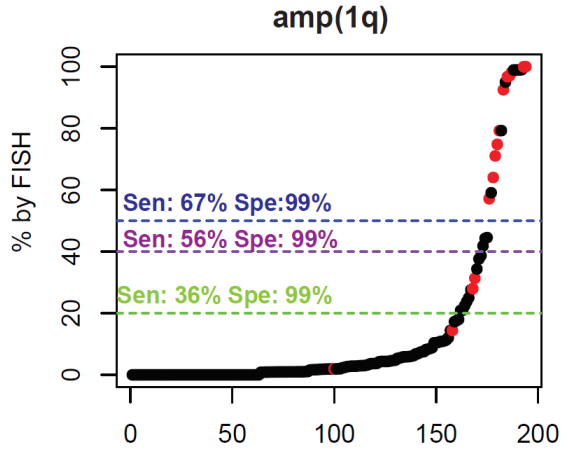


**Supplemental Figure 4: Validation of Copy Number Metrics Sequencing vs. FISH copy number calling** for A. gain or amp (1q)(*CKS1B*), B. amp(1q)(*CKS1B*) C. del(1p) (1p13 FISH probe compared to *FAM46C* (1p12) deletion), A. del(17p)(*TP53*)

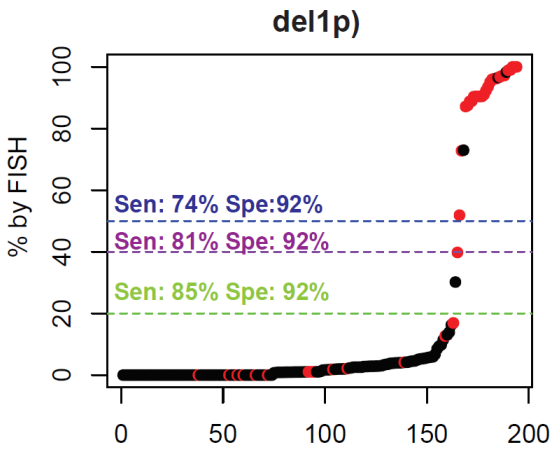
A.



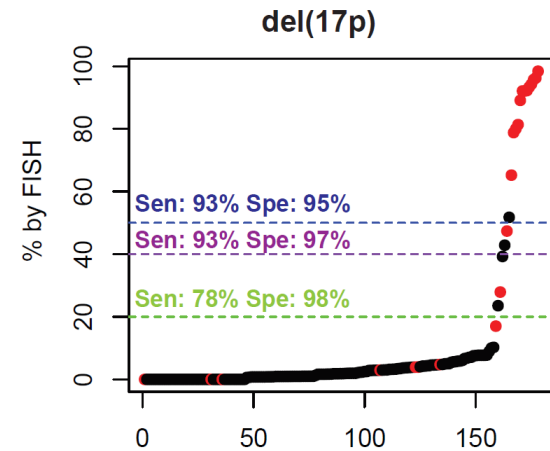
B.



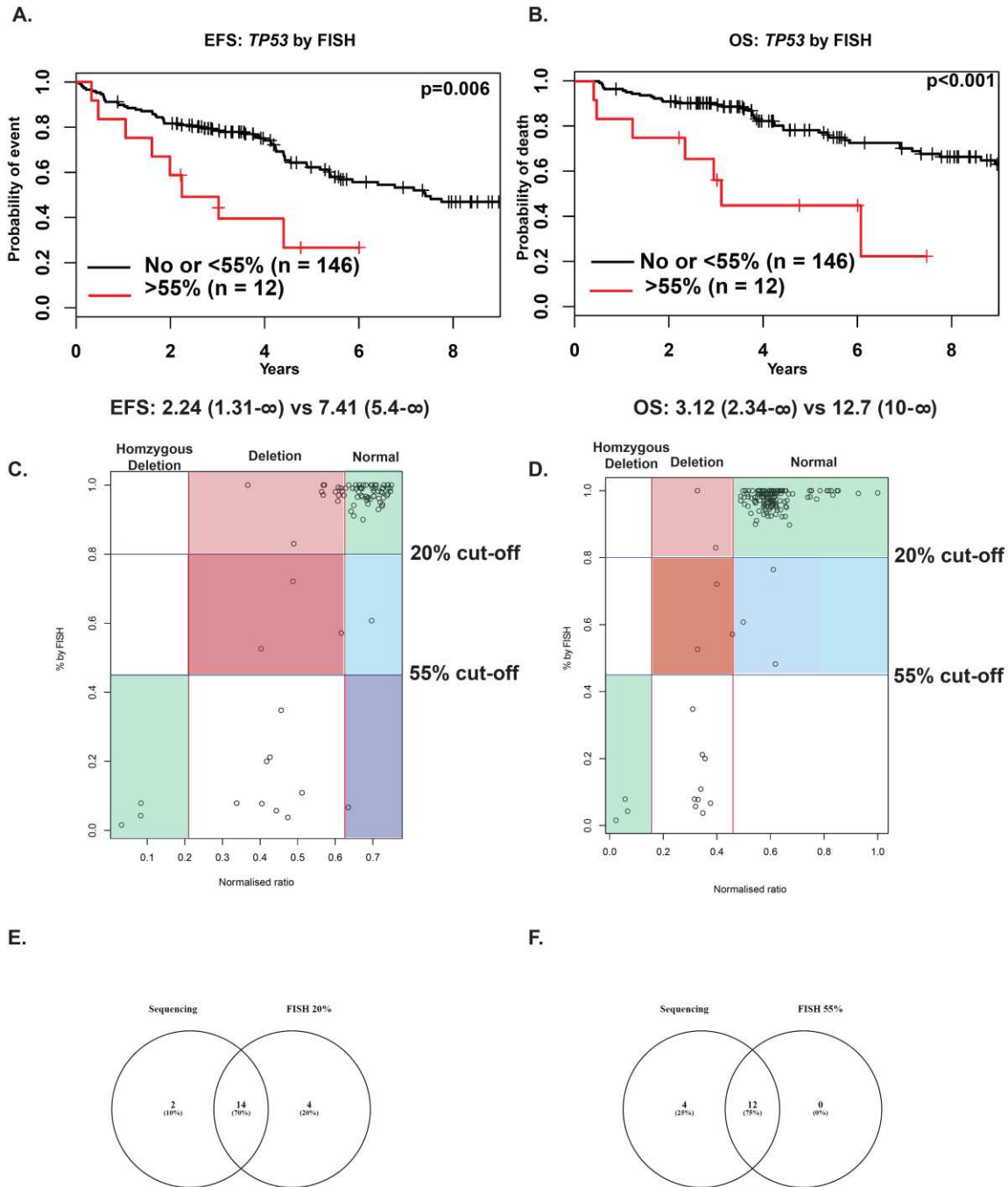
C.



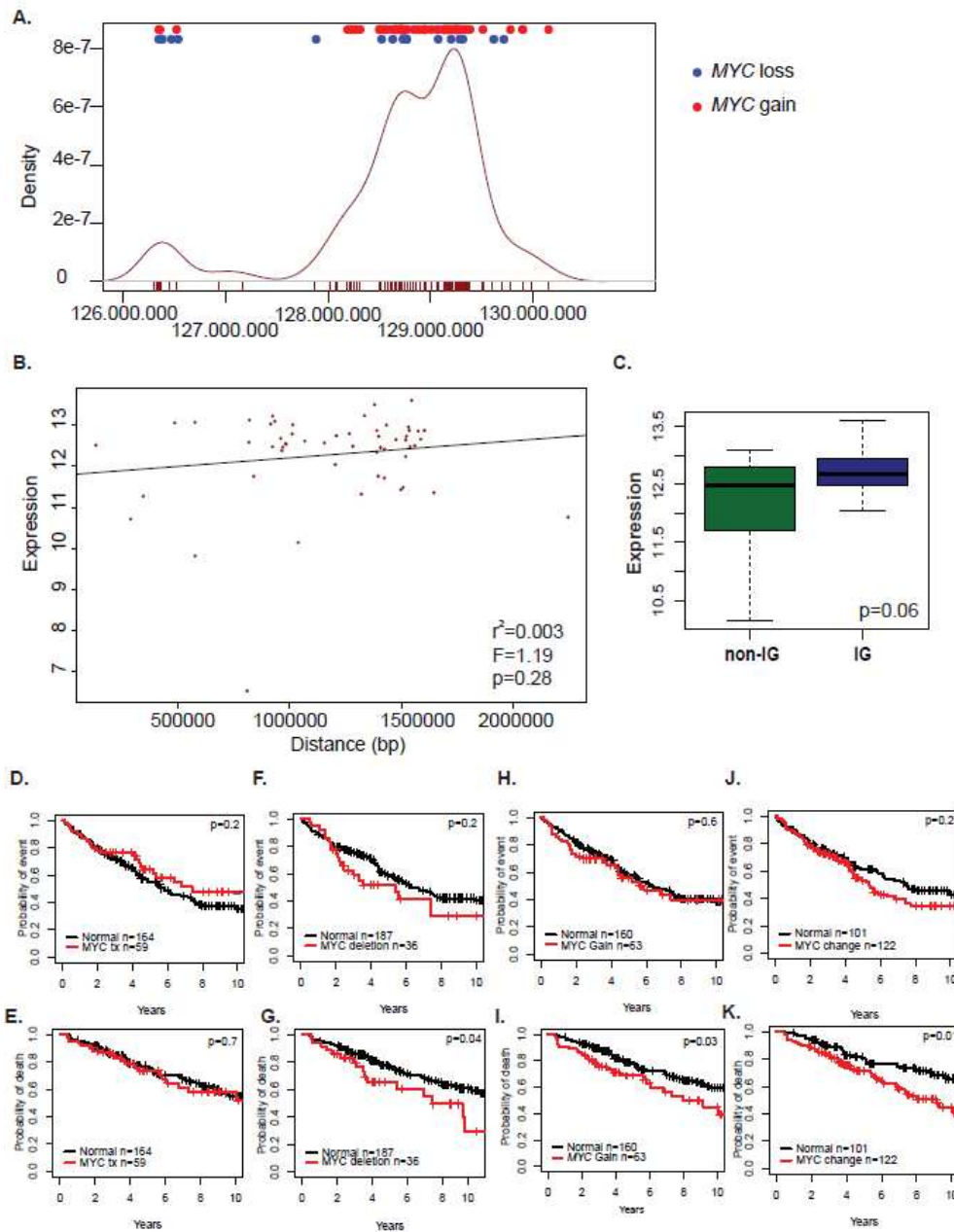
D.



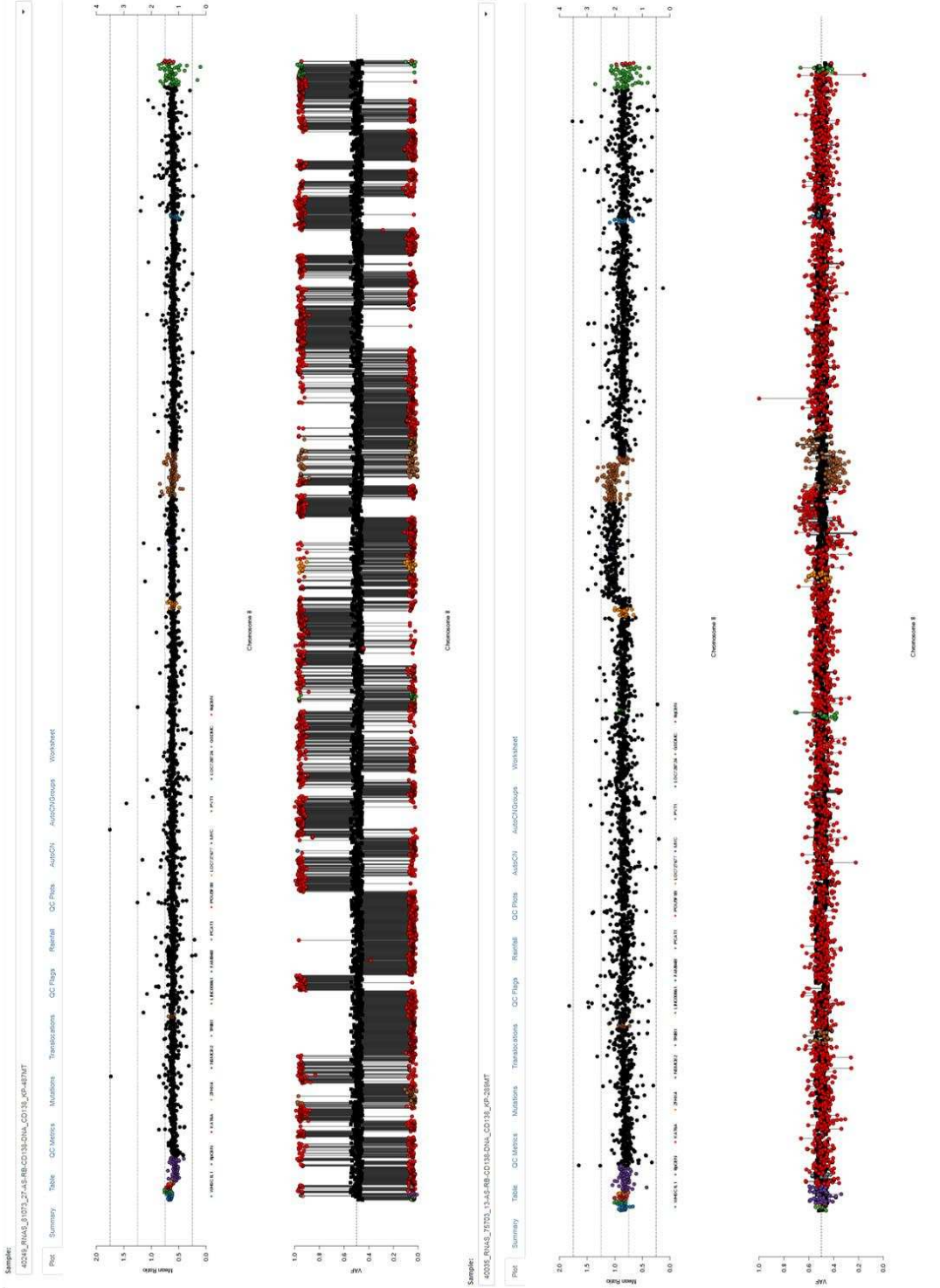
**Supplemental Figure 5: Validation of Copy number changes (*TP53*).** Using a 55% cut-off for *TP53* loss by FISH is prognostic on EFS (Panel A) and OS (Panel B). By using the non-normalized ratio (Panel C) there are many false positives (pink: 20% cut-off, red: 55% cut-off) and false negative (light blue 20% cut-off and navy blue 55% cut-off). By choosing the chromosome with the least variance as reference, normalized ratio are corrected and FP/FN rates decrease (Panel D). Overlap between diagnostic methods and cut-offs are presented on Panel E and F.



**Supplemental Figure 6: MYC rearrangements.** A. Density plot featuring the breakpoint on 8q24 consistent with the three hotspot previously published. Above, correspondence between the breakpoints and co-occurring MYC loss or gain. B. Correlation between distance from MYC and expression suggesting there is no correlation C. Difference in expression between IG and non-IG translocations. D-K. Impact of MYC changes on outcome: IG MYC translocations (D. EFS, E=OS), Deletions (F=EFS, G=OS), Gain (H=EFS, I=OS), and any change (J=EFS, K=OS).

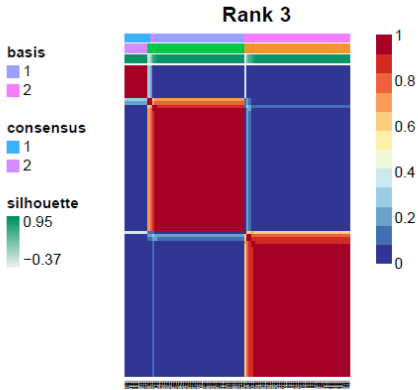


**Supplemental Figure 7: Example of MYC rearrangements. A. Deletion on 8q B. Gain of part of 8q24 as visualized by the chromosome viewer.**

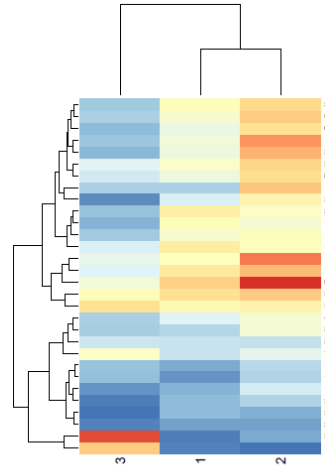


**Supplemental Figure 8: nNMF: signatures.** A. Rank=3 was the best ranking option. B There are two background signature within the same clade and an APOBEC (2,13) signature C. Background signature, D. Background signature, E. APOBEC signature (2 and 13).

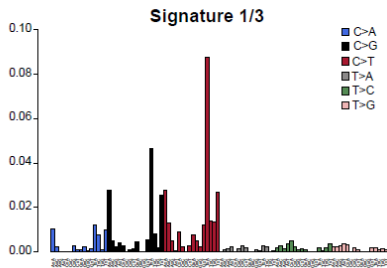
A.



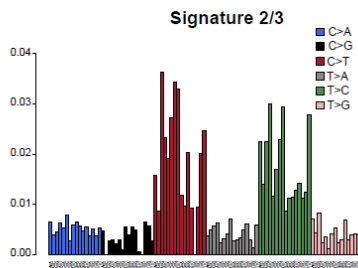
B.



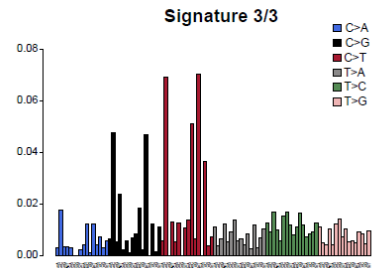
C.



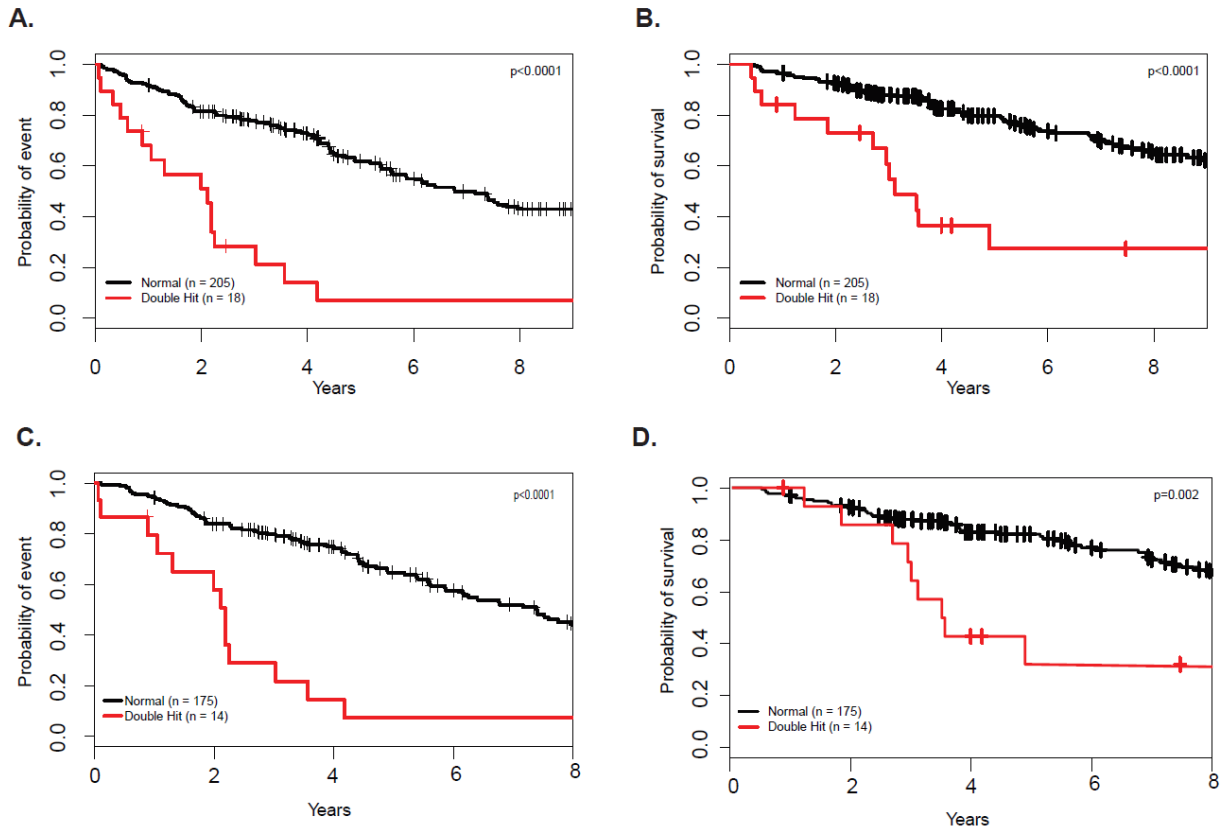
D.



E.

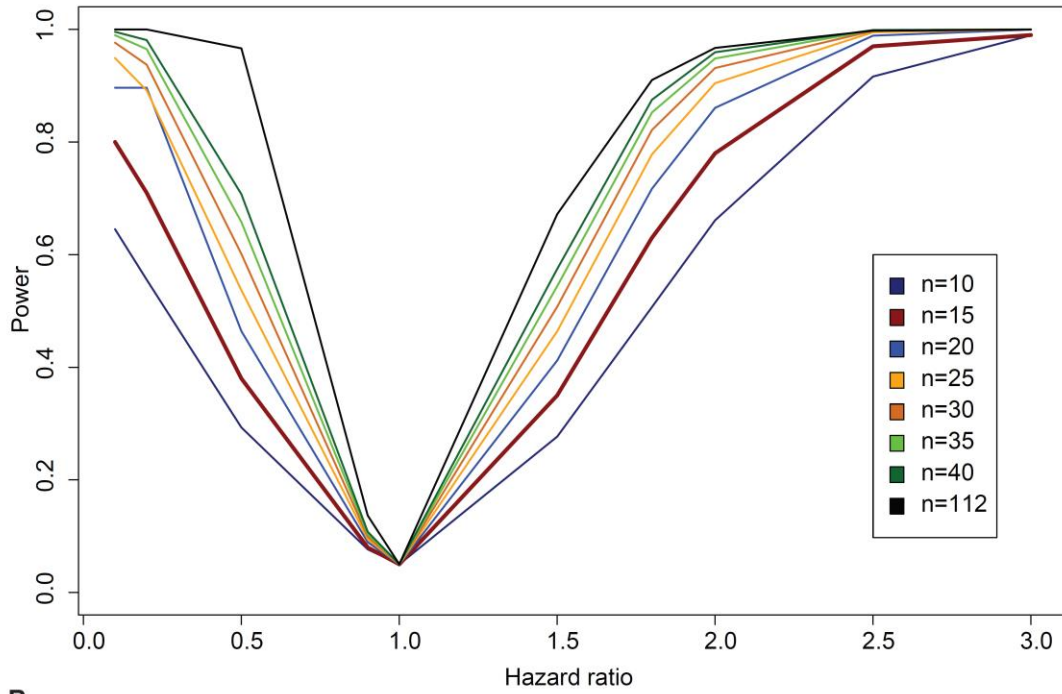


**Supplemental Figure 9: Impact of Double-Hit on outcome. A. EFS B. OS C. EFS in the Intention to treat (ITT) population and D. OS in the ITT population.**

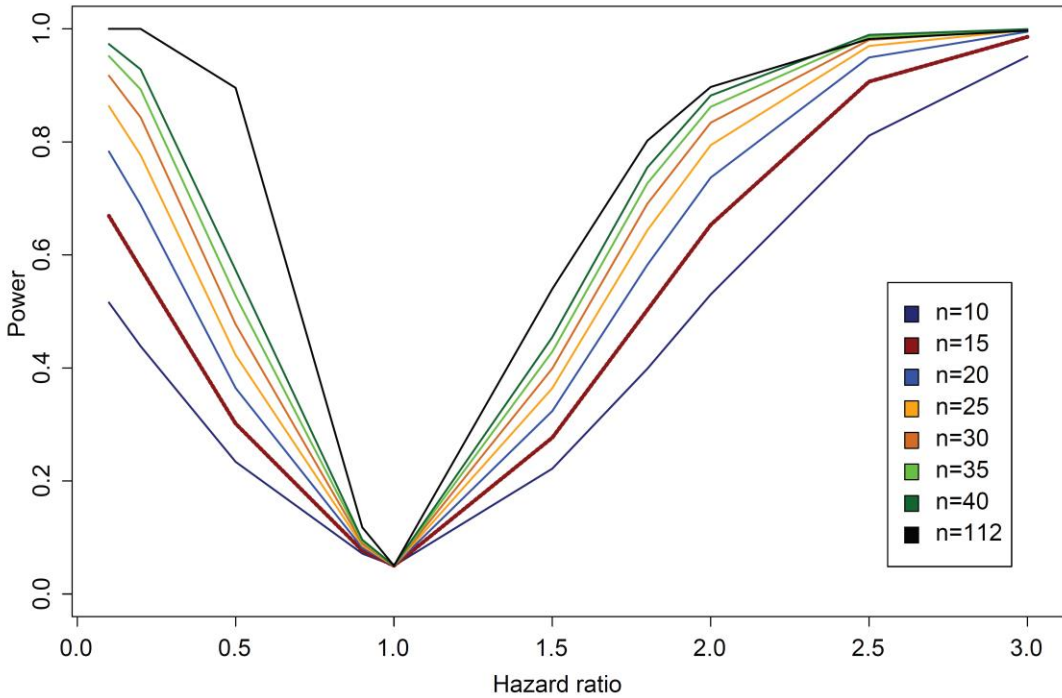


**Supplemental Figure 10: Power analysis for EFS and OS based on group size given the 8-year follow-up.**

**A.**

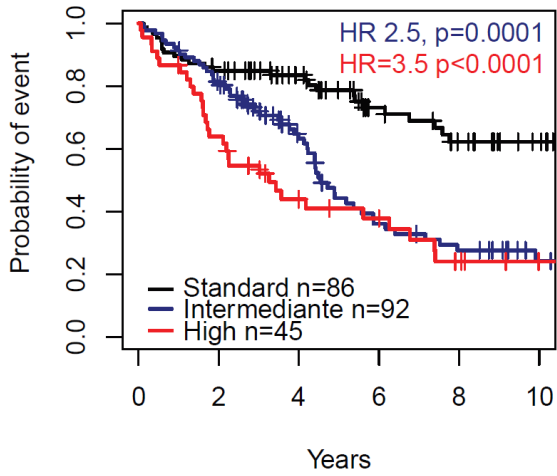


**B.**

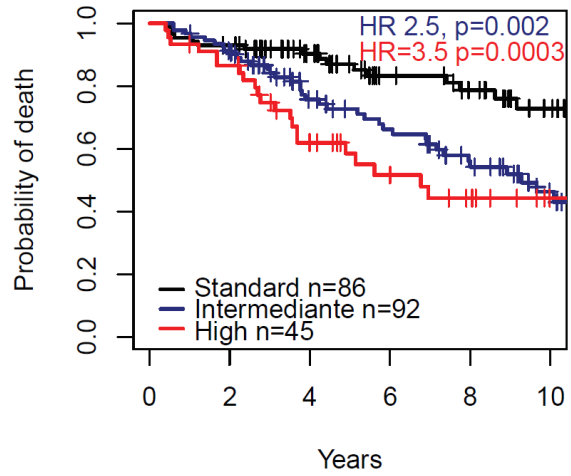


**Supplemental Figure 11: Impact of current survival models on outcome in this dataset. IFM2009 model on EFS (A.) and OS (B). GEP70 score on EFS (C) and OS (D).**

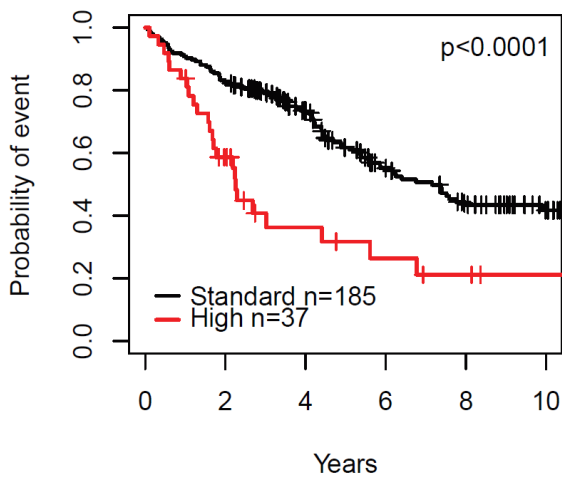
**A.**



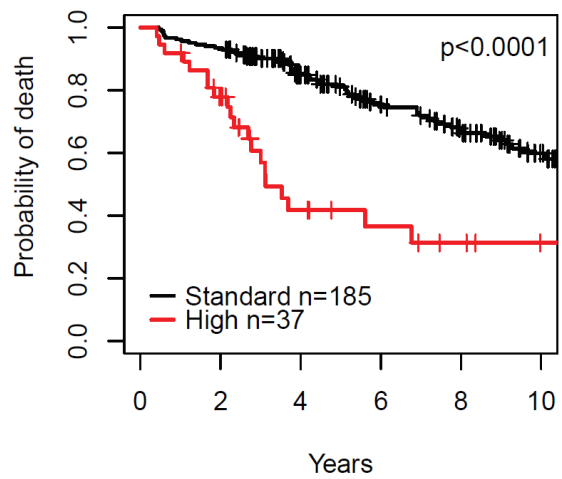
**B.**



**C.**

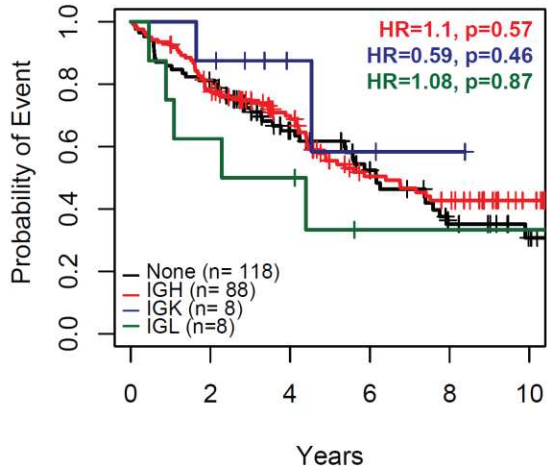


**D.**

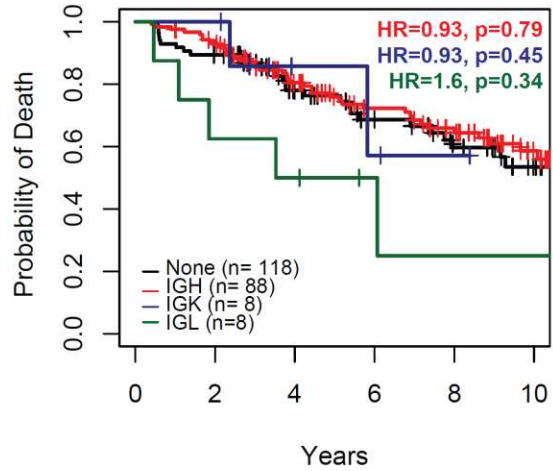


**Supplemental Figure 12: Impact of translocation partners. A EFS B. OS C. Impact of t(4;14) depending on the presence of a DIS3 mutation on EFS**

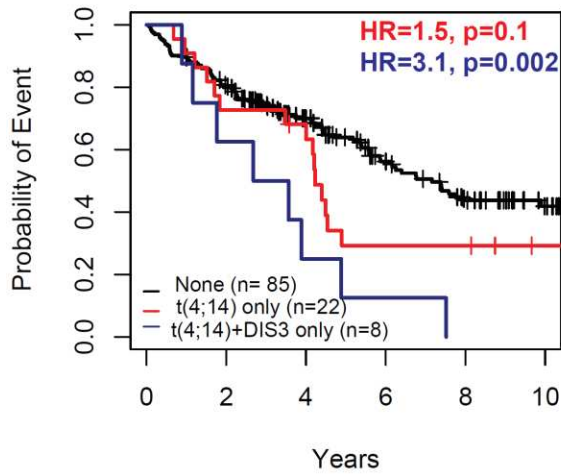
**A.**



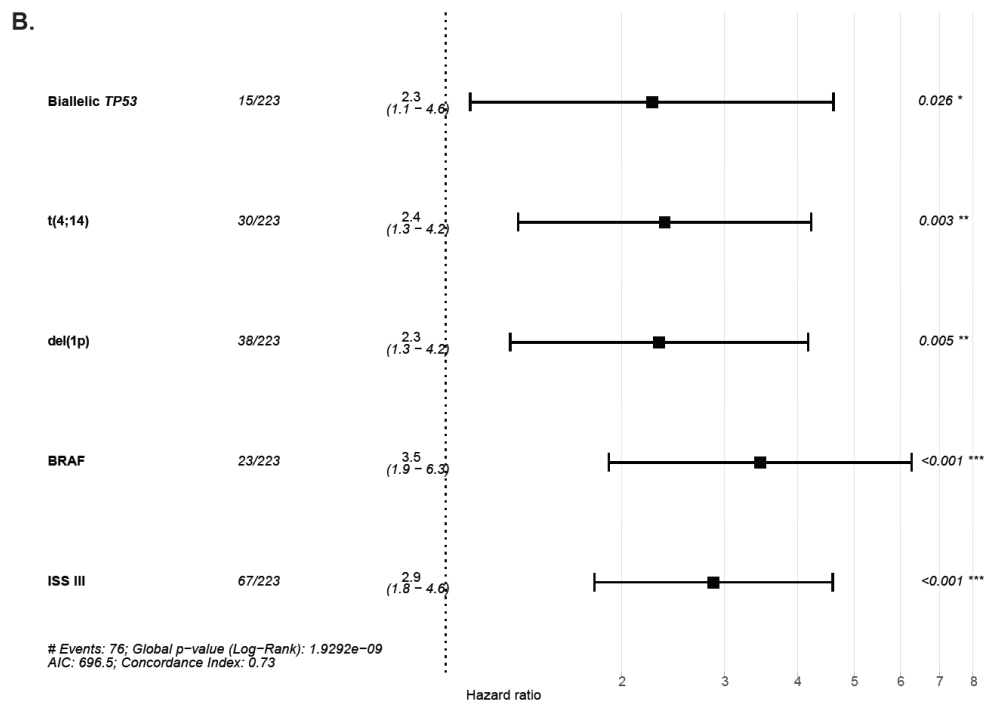
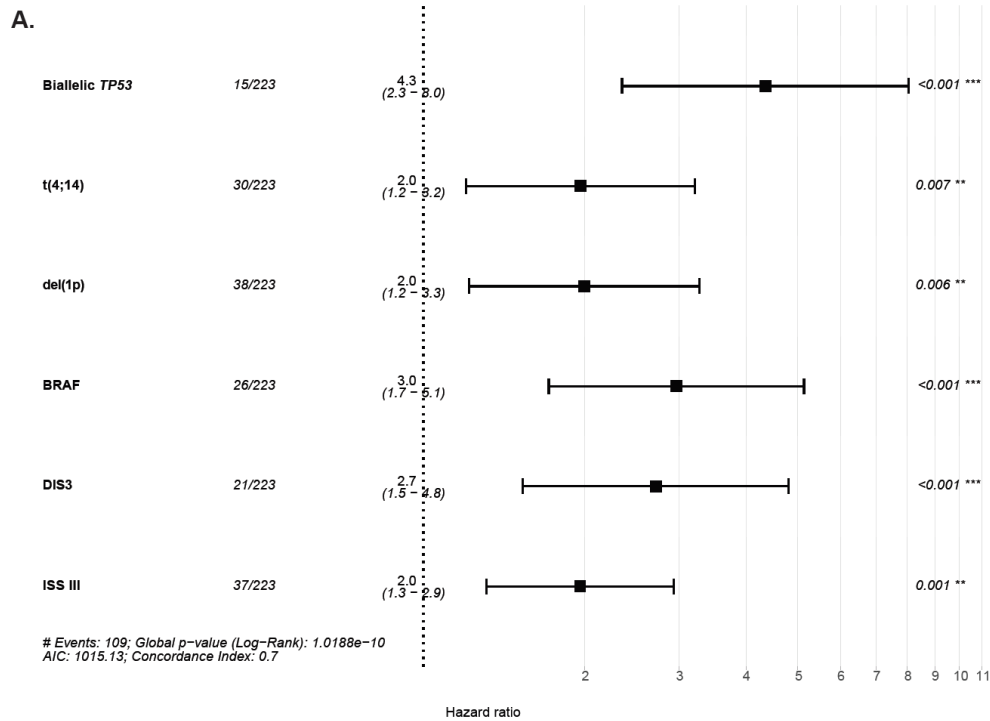
**B.**



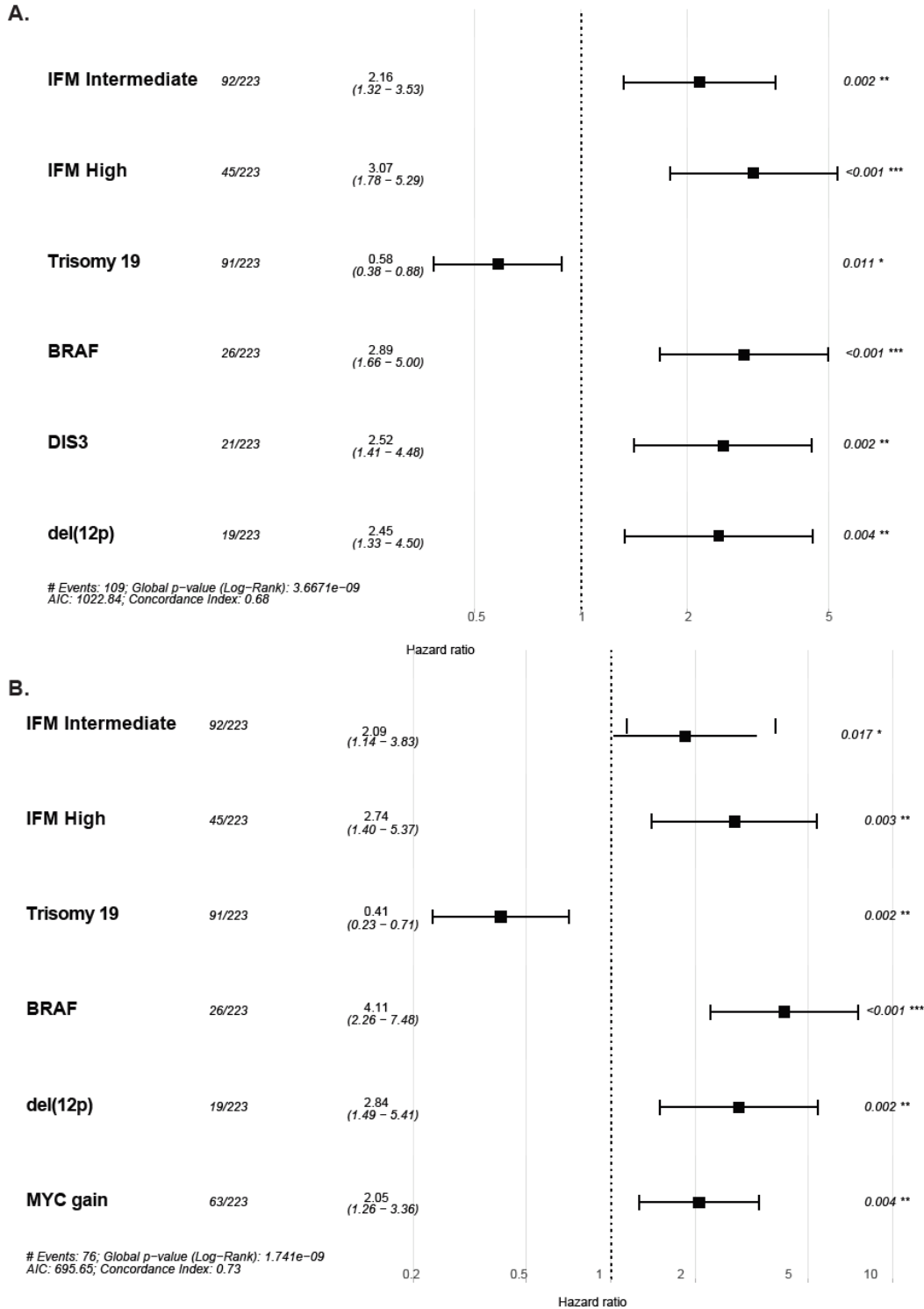
**C.**



**Supplemental Figure 13: Multivariate analysis using common risk factors.** We performed a “cherry picking approach where we included all the classic prognostic features (Biallelic *TP53*, t(4;14), del(1p), gain(1q), ISS, HRD, *MYC* translocations) alongside the new features we identified (*BRAF* and *DIS3* mutations, del(12p)) and analyzed the impact on A. EFS B. OS.

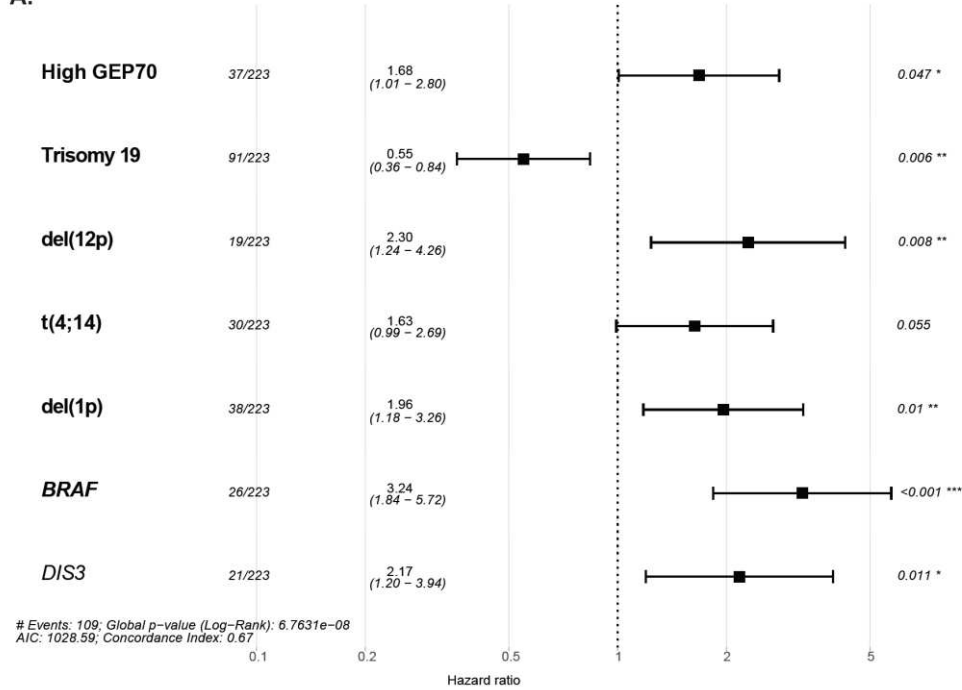


**Supplemental Figure 14: Multivariate analysis IFM model.** We performed a unbiased approach where we included IFM model (based on t(4;14), del(1p), gain(1q), del(17p), Trisomy 21, Trisomy 5) alongside the features with p<0.1 excluding ISS , DH, and GEP70 and analyzed the impact on A. EFS B. OS..

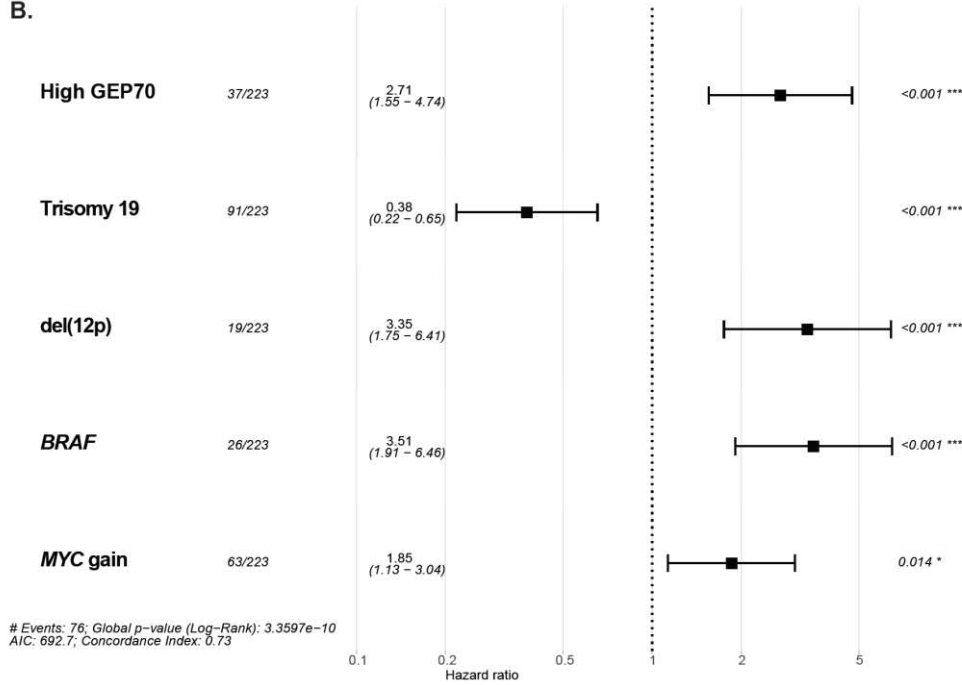


**Supplemental Figure 15: Multivariate analysis GEP70 model.** We performed an unbiased approach where we included the GEP70 score alongside all features with a  $p < 0.1$  except ISS and Double-Hit (including Bi-allelic TP53) and analyzed the impact on A. EFS B. OS.

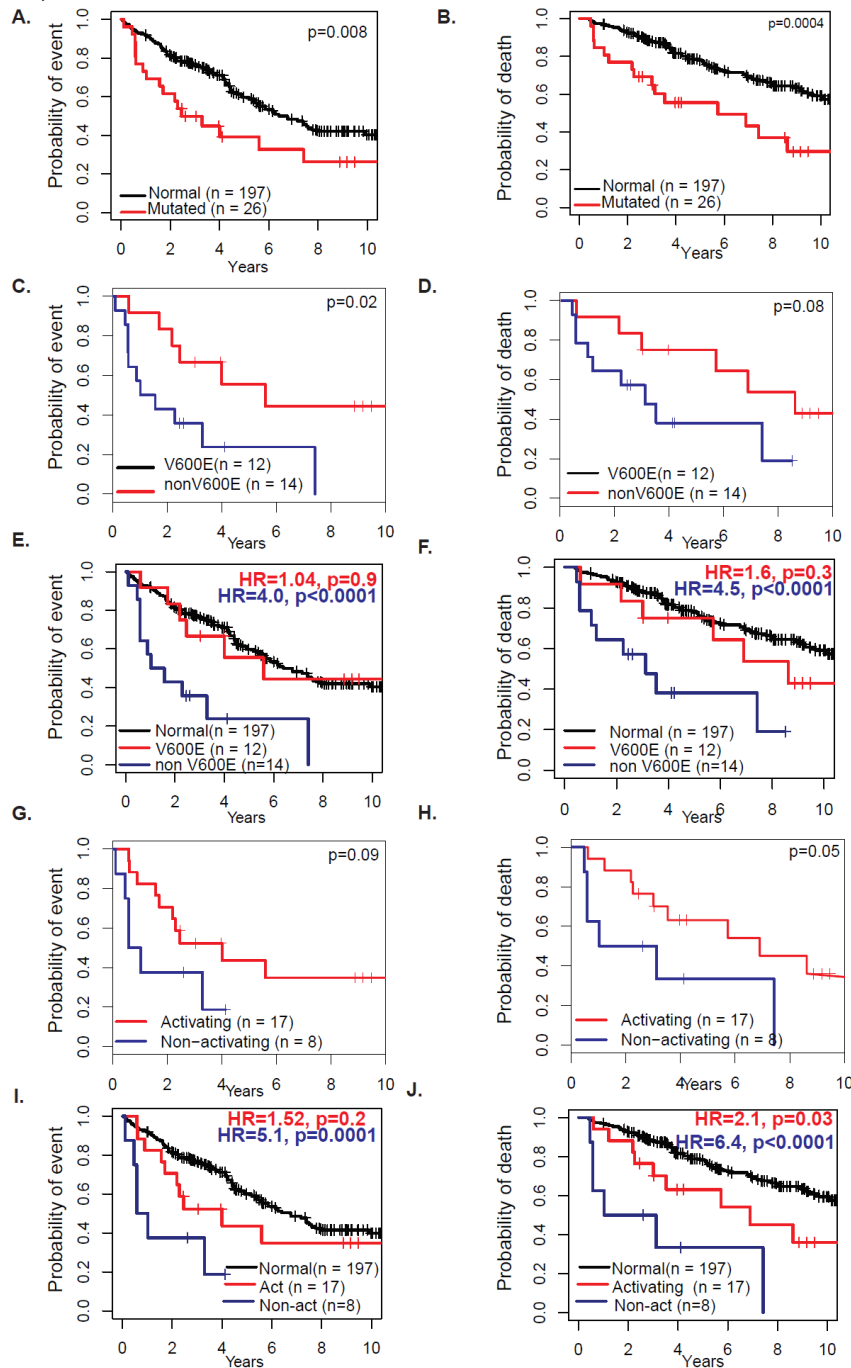
A.



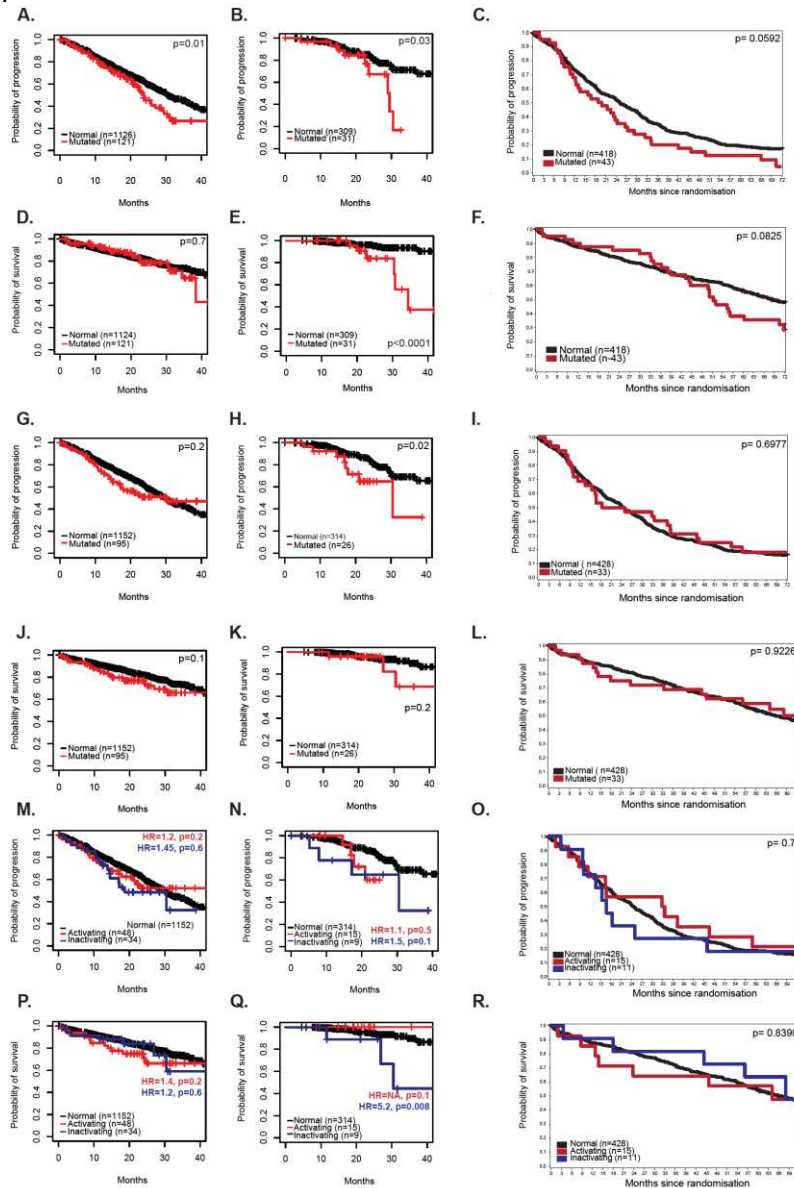
B.



**Supplemental Figure 16: Impact of BRAF on outcome.** A. Impact of BRAF mutations on EFS (A) and OS (B). Differential impact of V600E and non-V600E mutations on EFS (C-E) and OS (D-F) Differential impact based on predicted BRAF function on EFS (G-I) and OS (H-J).

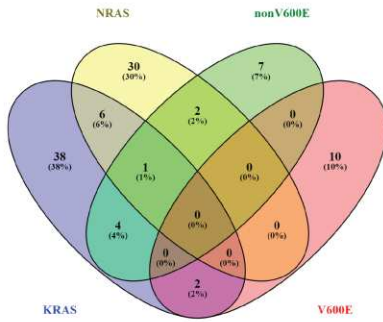


**Supplemental Figure 17: Validation of mutations in the MGP complete dataset (n=1274), MGP intensively treated patients (n=340) and Myeloma XI patients only (n=463).** Impact of *DIS3* mutations on PFS in the A. MGP complete dataset, B MGP intensively treated patients and C Myeloma XI patients; OS in D. MGP complete dataset, E MGP intensively treated patients and F. Myeloma XI patients. Impact of *BRAF* mutations on PFS in the G. MGP complete dataset, H MGP intensively treated patients and I Myeloma XI patients; OS in J. MGP complete dataset, K MGP intensively treated patients and L. Myeloma XI patients. Impact of *BRAF* mutation's function on PFS in the M. MGP complete dataset, N MGP intensively treated patients and O Myeloma XI patients, OS in P. MGP complete dataset, Q MGP intensively treated patients and R. Myeloma XI patients.

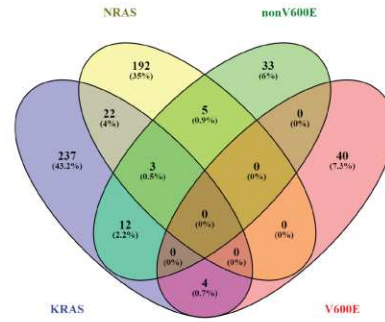


**Supplemental Figure 18: Co-segregation of *BRAF*, *KRAS*, and *NRAS* mutations.** Venn diagrams representing the co-segregation of mutations in this (A) and the MGP (B) datasets. Respective CCFs of each mutation suggest at least half of them are in the same clones in this (C) and the MGP (D) datasets.

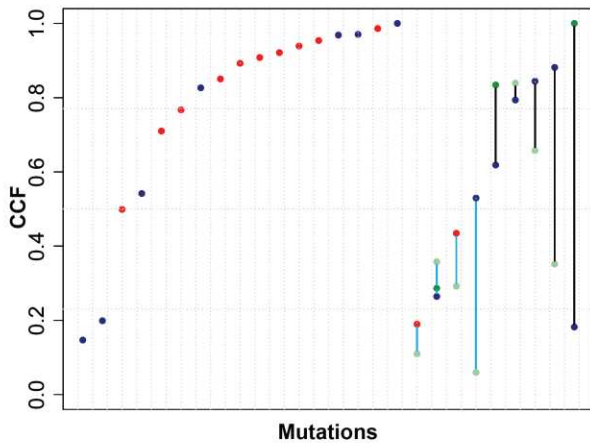
A.



B.

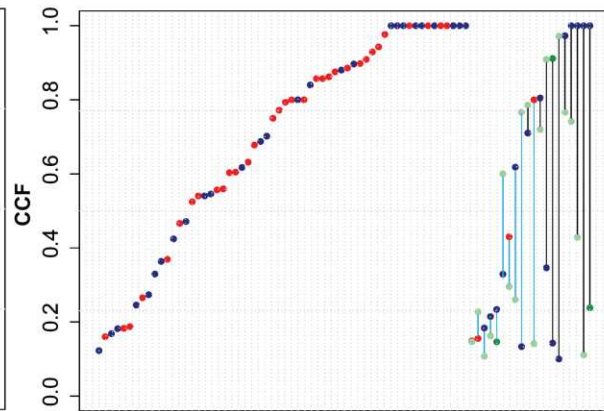


C.



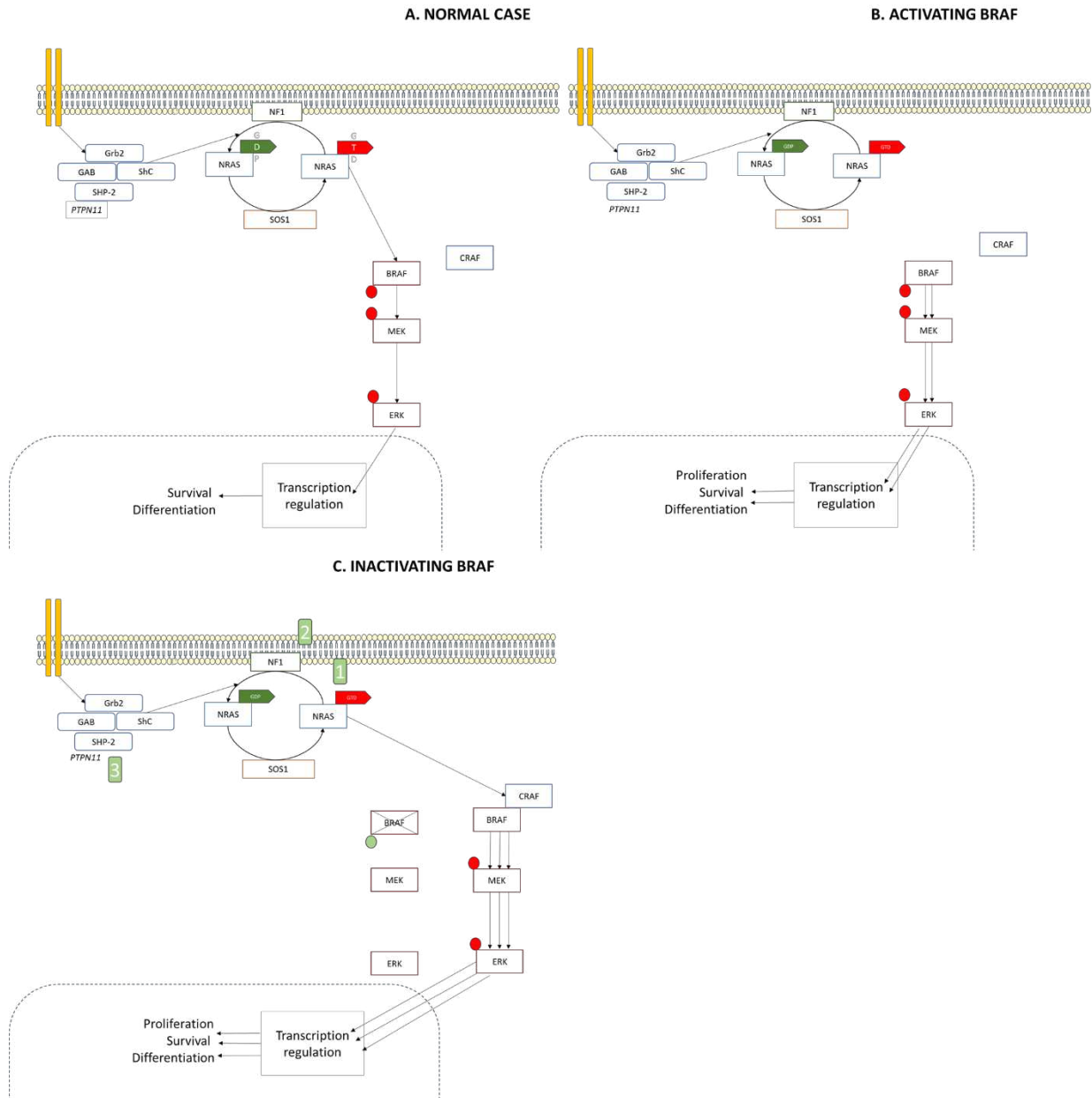
• *BRAF* non-V600E    • *KRAS*    — Same clone  
 • *BRAF* V600E        • *NRAS*    — Undetermined clonality

D.



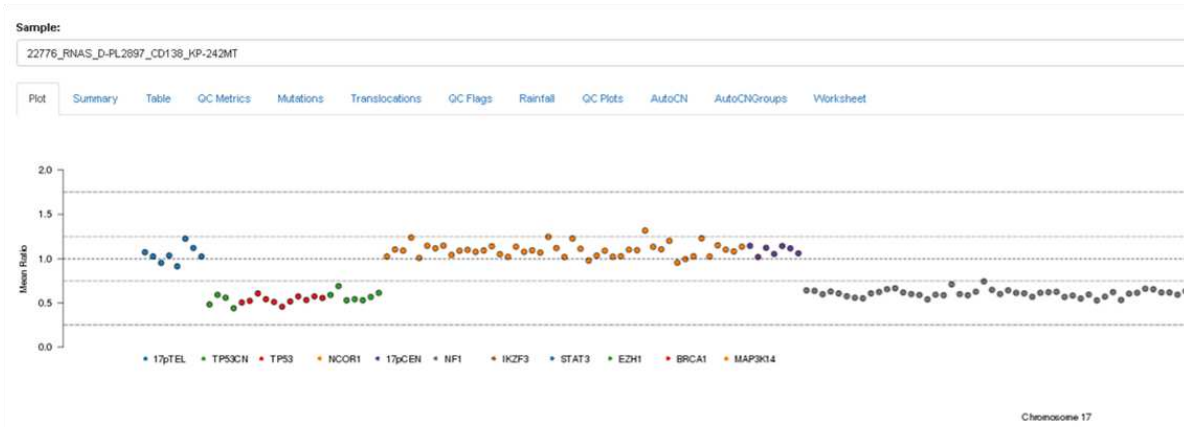
• *BRAF* non-V600E    • *KRAS*    — Same clone  
 • *BRAF* V600E        • *NRAS*    — Undetermined clonality

**Supplemental Figure 19: MAPK pathway. A.** In the physiological case, upon a signal from the receptor, SHP2 proteins, NRAS or KRAS, hydrolyse to phosphorylate BRAF and activate the downstream MAPK pathway leading to survival and differentiation. This reaction is regulated by GAPS and GEFs such as RASA1 and NF1. **B.** In case of an activating BRAF mutation, MAPK activation becomes independent from upstream signal and regulation. **C.** In the case of an inactivating mutation, BRAF can dimerize with CRAF and lead to hyperactivation of the MAPK pathway, thus leading to a survival advantage. A second “hit” is believed to be required. In melanoma it has been shown to be bi-allelic loss of NF1 or PTPN11, in NSCL it can be EGFR mutations, in both diseases like what we hypothesize in MM it is KRAS or NRAS mutations.



**Supplemental Figure 20: Examples of *TP53* deletions.** A. Loss of *TP53*. B. Interstitial deletion of the 5' end of *TP53* leading to a biallelic inactivation of the gene.

**A.**



**B.**

